The rocky path to geomechanics
A geologist's tale

Martin P. J. Schöpfer

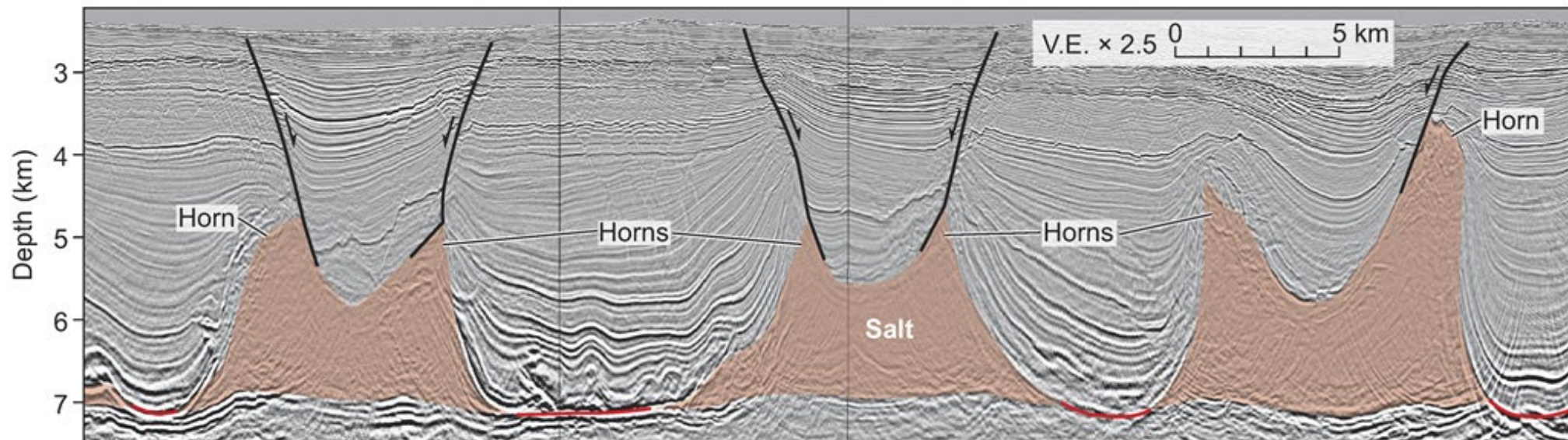*Department for Geodynamics and Sedimentology, University of Vienna, Austria.*

Growth of normal faults in mechanically layered sequences
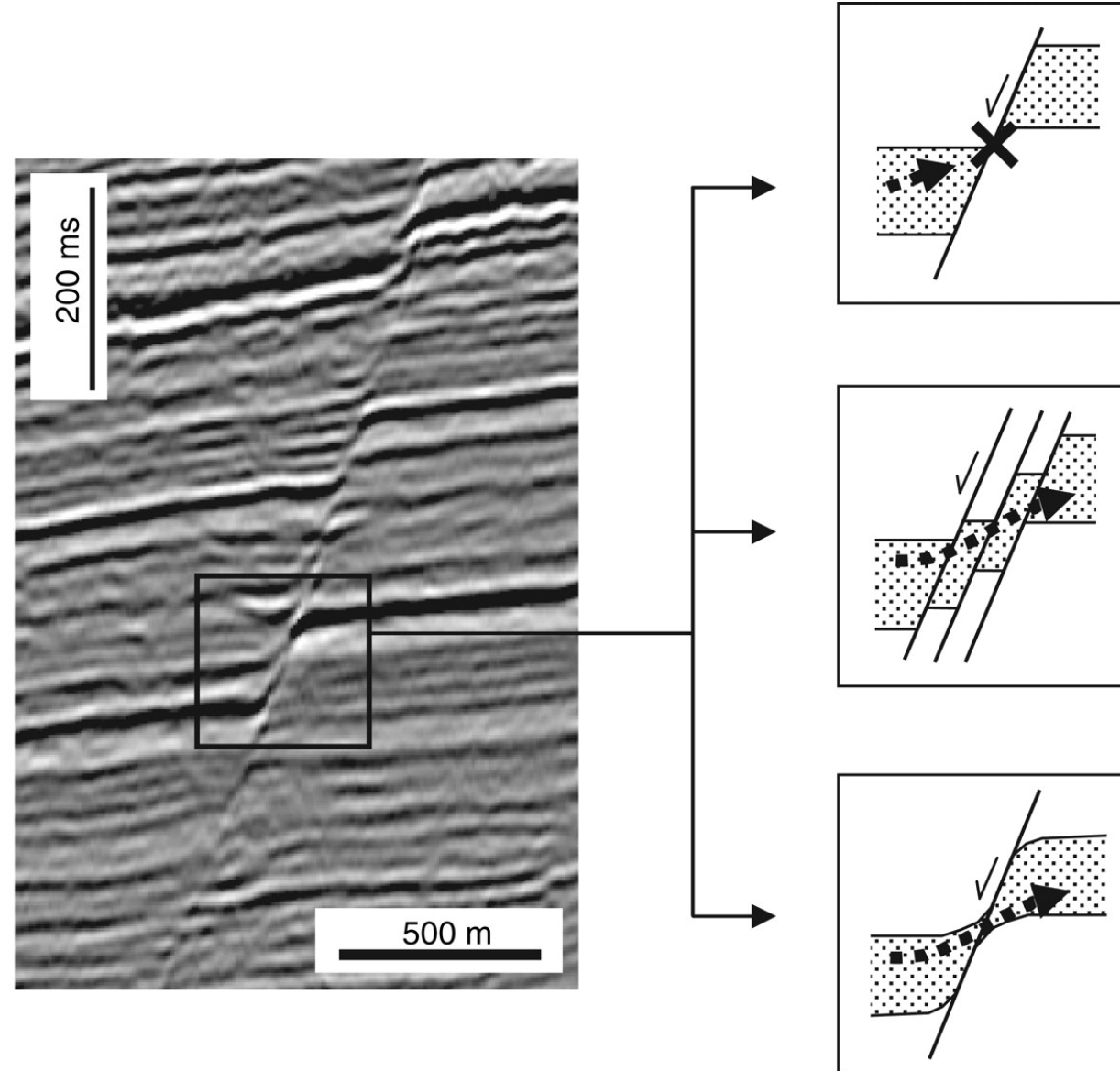

Mechanical controls on the spacing of rock joints

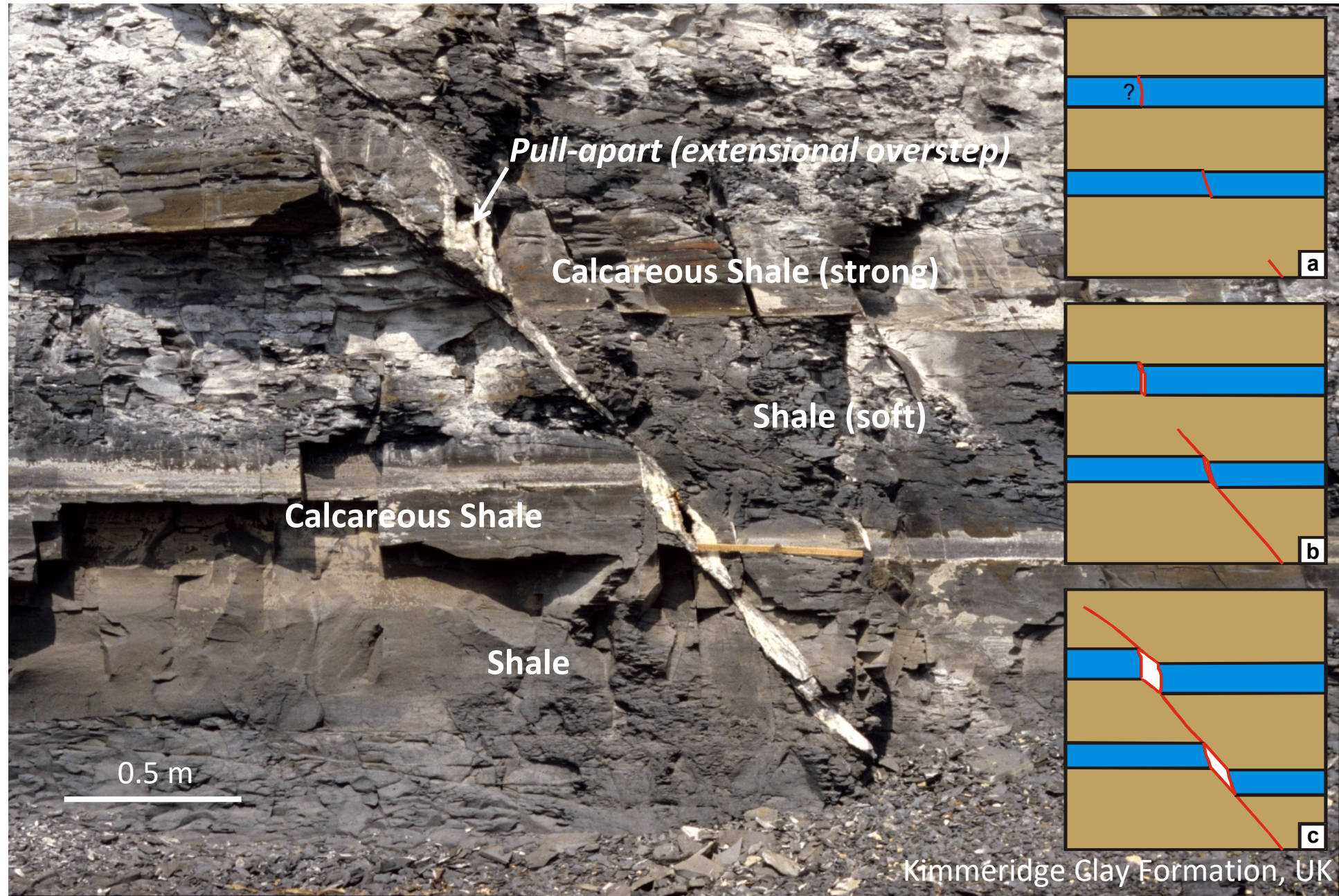# Formation of salt withdrawal basins under thin-skinned extension

# Farewell from the Fault Analysis Group, Dublin, April 2011

The problem of resolution from seismically imaged faults

Wibberley et al. (2008)

Example of a normal fault with layer-controlled fault dips

Pull-apart (extensional overstep)

Calcareous Shale (strong)

Shale (soft)

Calcareous Shale

Shale

0.5 m

Kimmeridge Clay Formation, UK

Schöpfer et al. (2006)

Refraction and segmentation of normal fault contained in limestone/shale sequence, Kilve, UK

strong

weak

strong

weak

1m

Schöpfer et al. (2007)
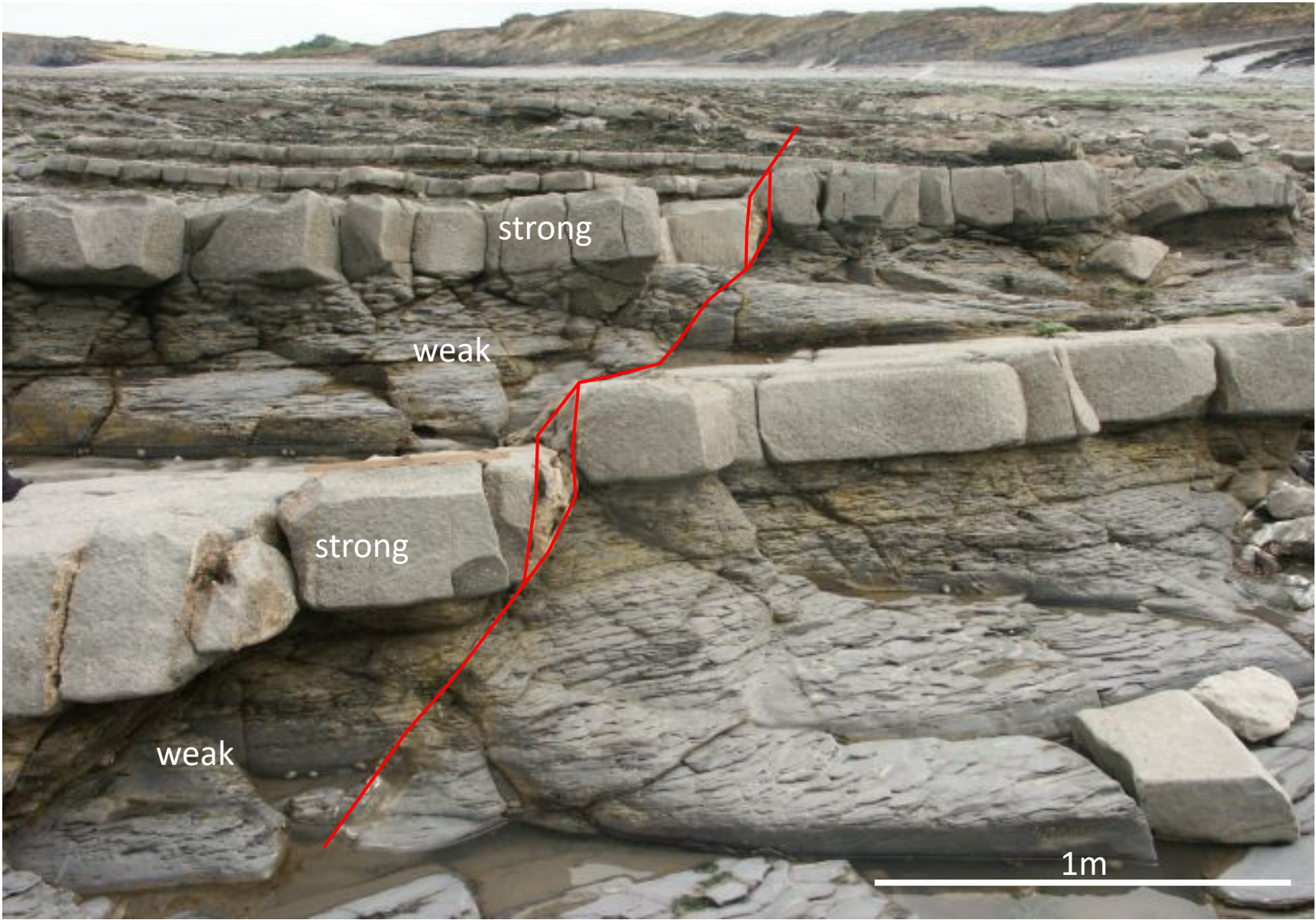
Theoretical fault trace of normal fault in mulitlayer as 'predicted' by Griffith and Coulomb-Mohr criterion


Schöpfer et al. (2009)
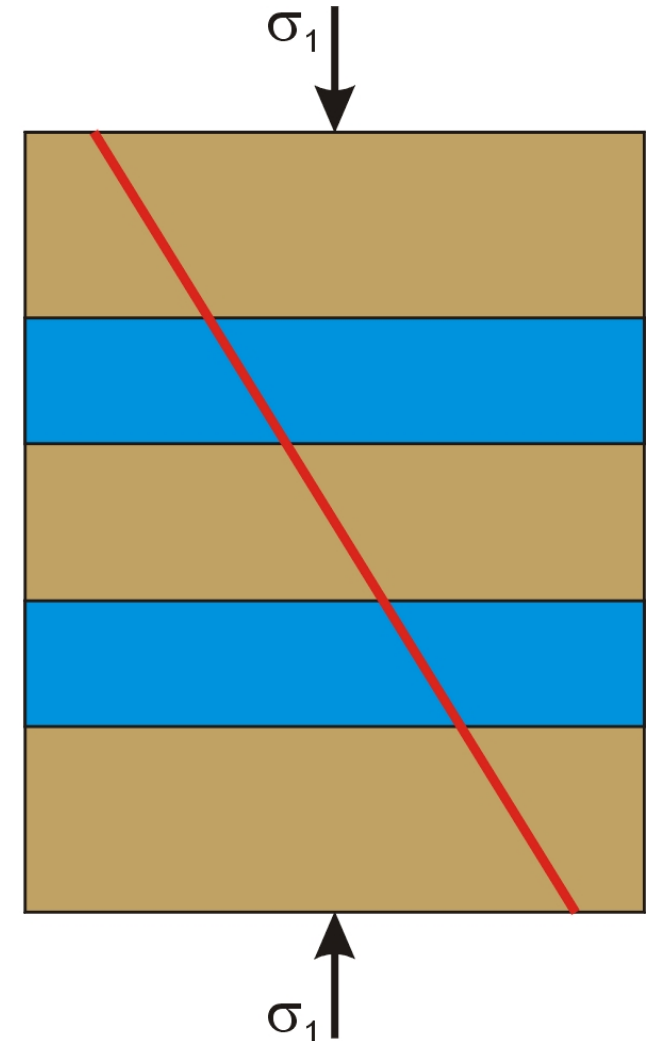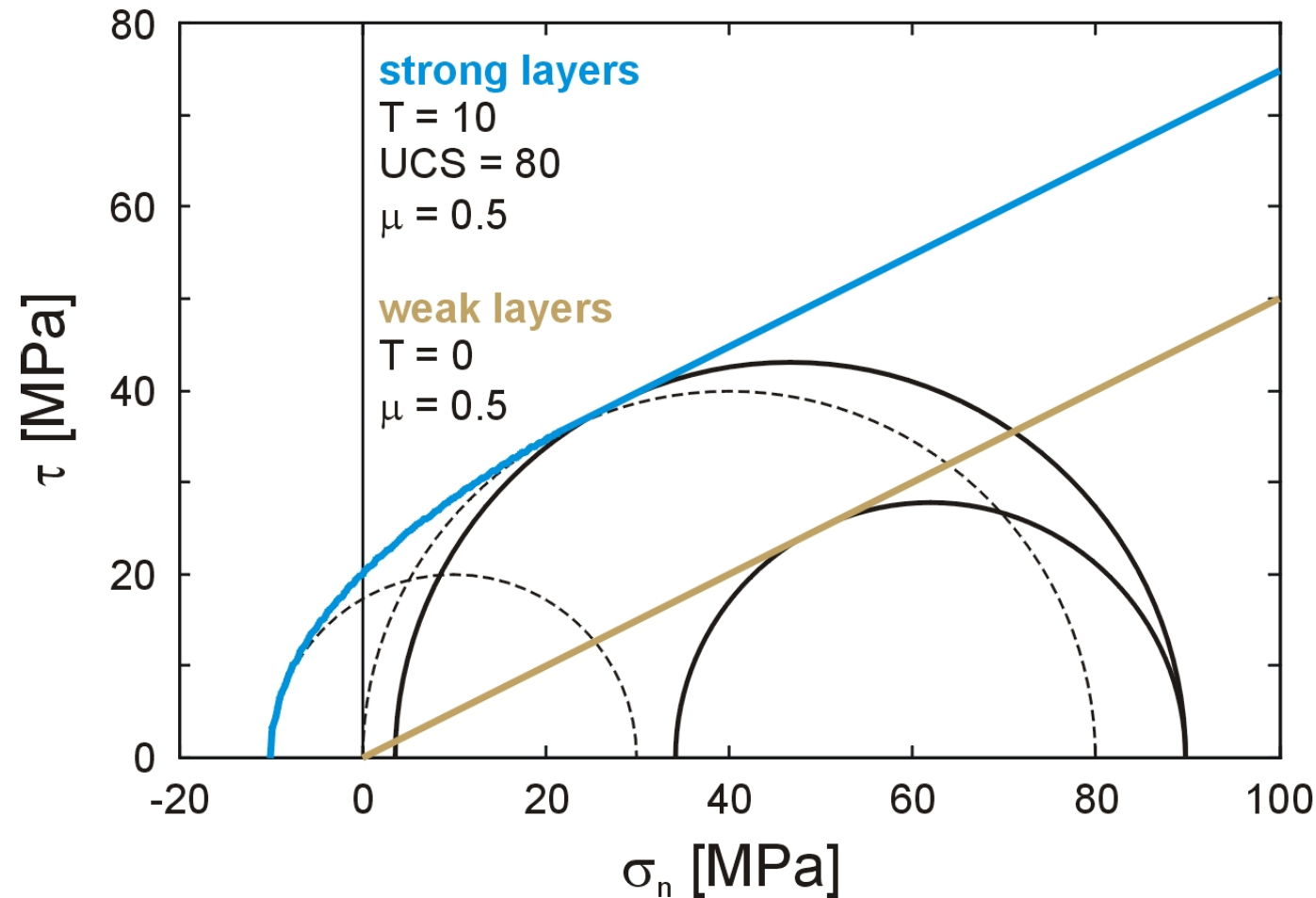
PFC2D modelling of normal faults in layered sequences

Normal faulting models are composed of strong layers (bonded particles) and weak layers (non-bonded particles) that are deformed in response to movement on a predefined fault at the base of the sequence, while a constant overburden pressure is maintained at the model top.

Schöpfer et al. (2006, 2007a, 2007b, 2009b)
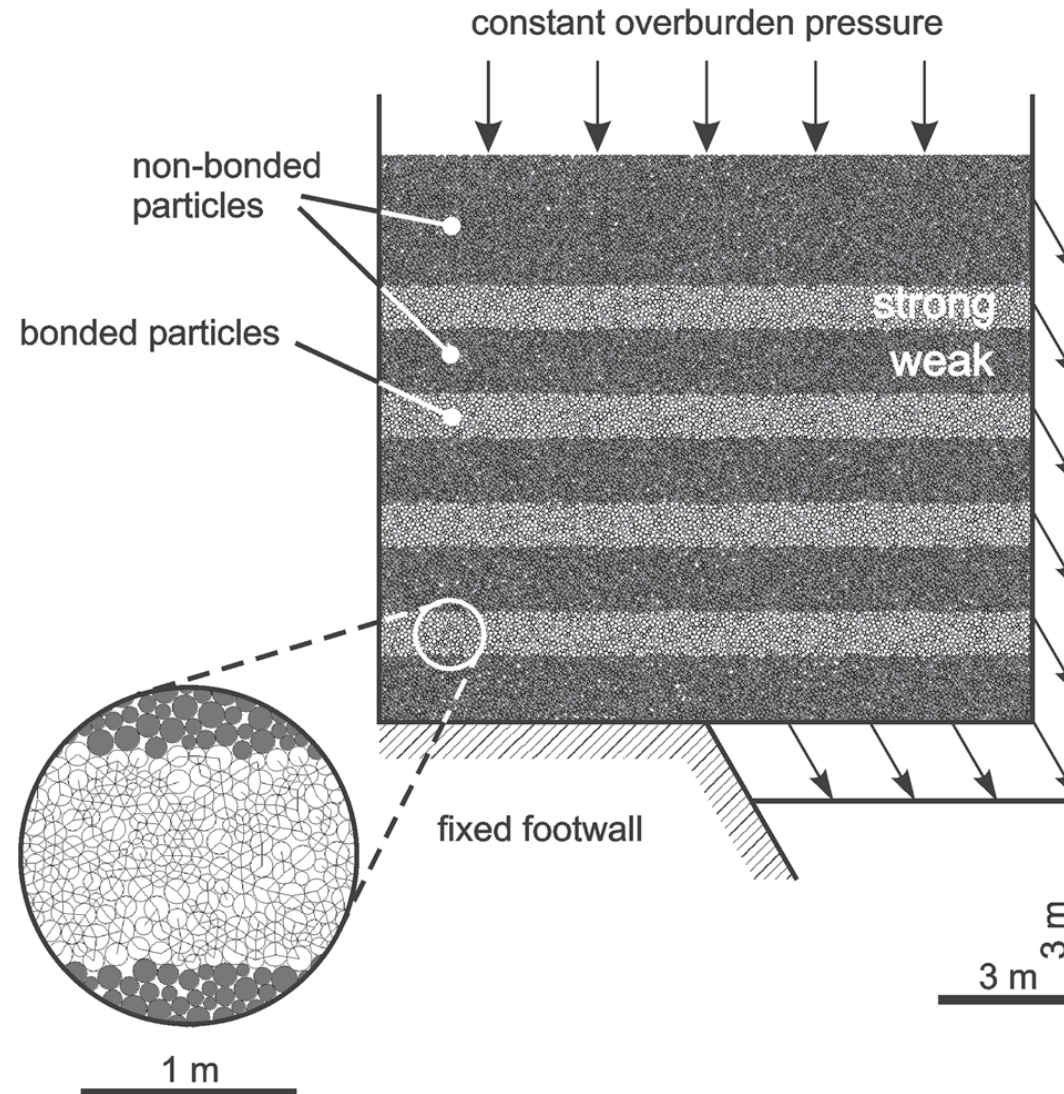
Prediction of fields of extension, hybrid and shear failure as a function of overburden pressure and strength
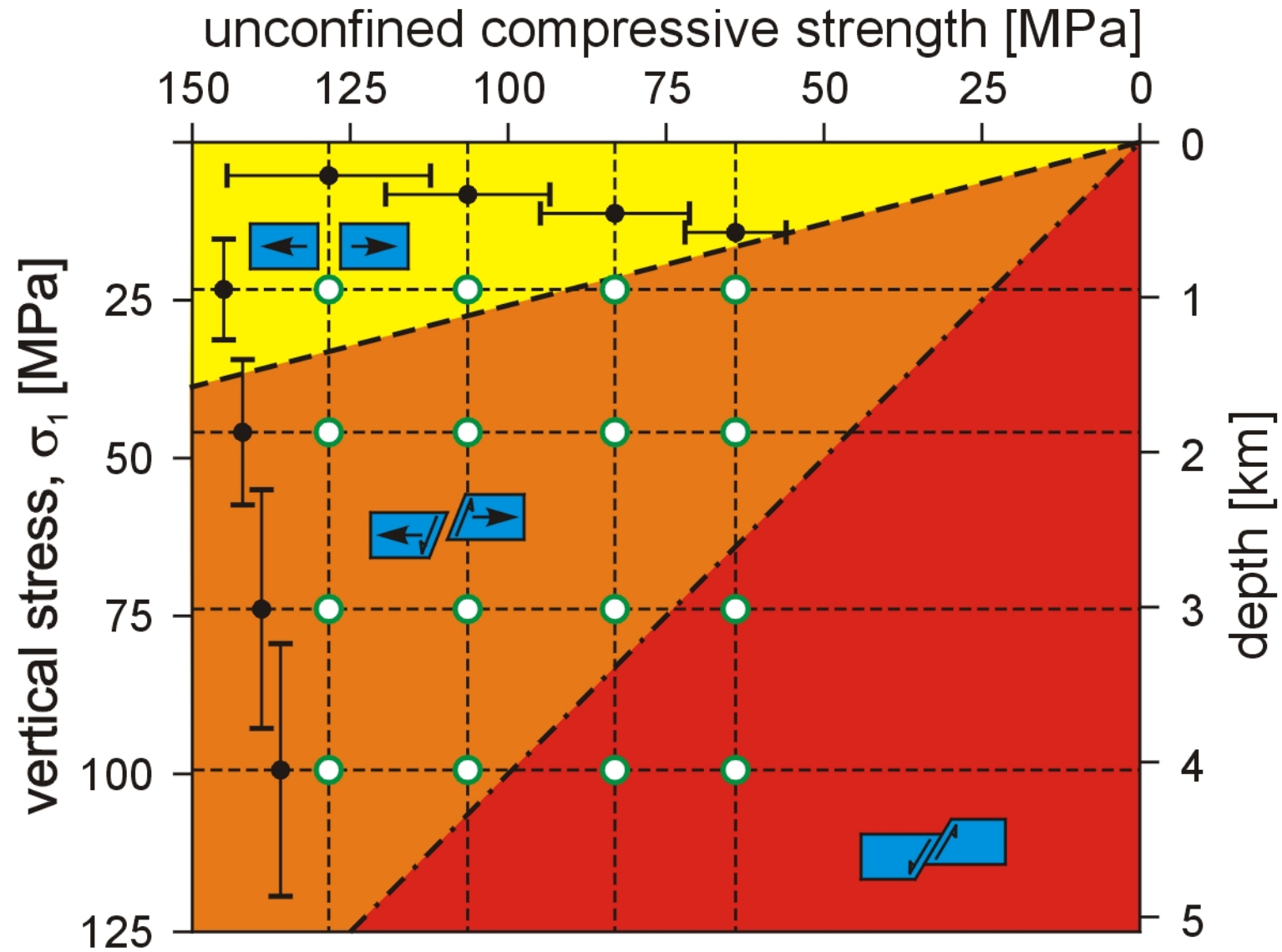
throw = 0.5 m

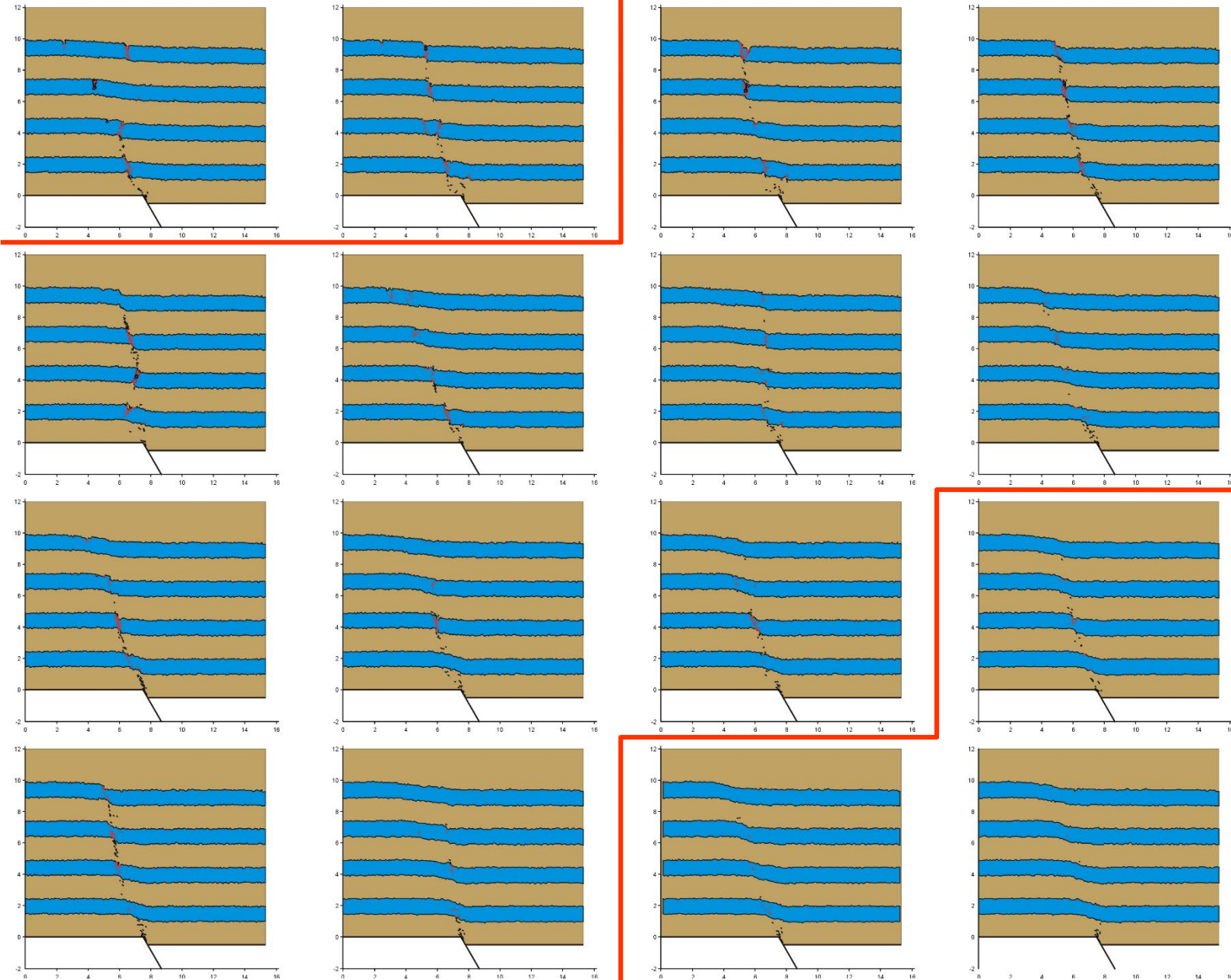## unconfined compressive strength

| | 128 MPa | 106 MPa | 83 MPa | 64 MPa |

depth of faulting

1 km

2 km

3 km

4 km

Schöpfer et al. (2007)

throw = 1.0 m

unconfined compressive strength

Schöpfer et al. (2007)

unconfined compressive strength

throw = 1.5 m

	128 MPa	106 MPa	83 MPa	64 MPa

depth of faulting

1 km

2 km

3 km

4 km
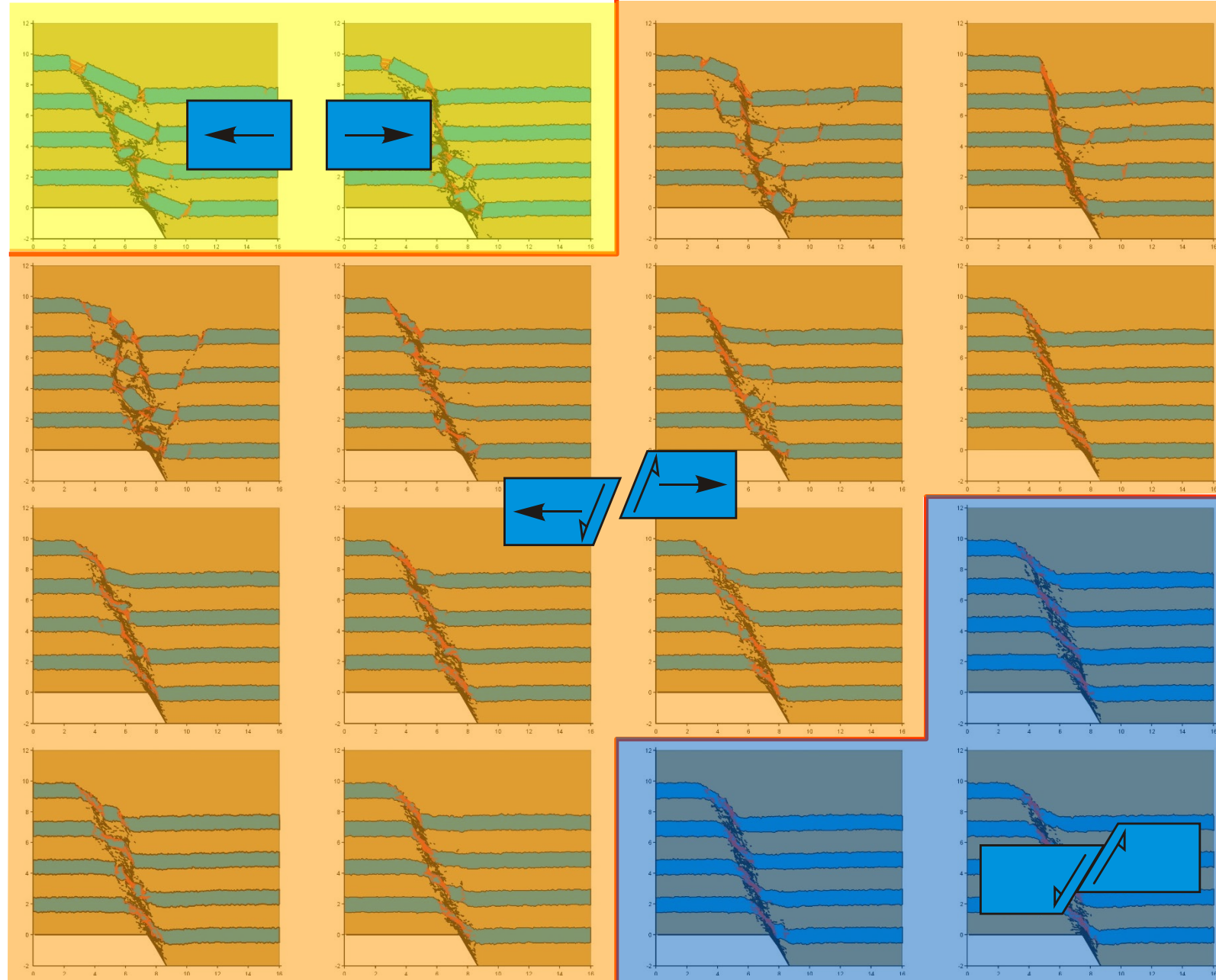
Schöpfer et al. (2007)
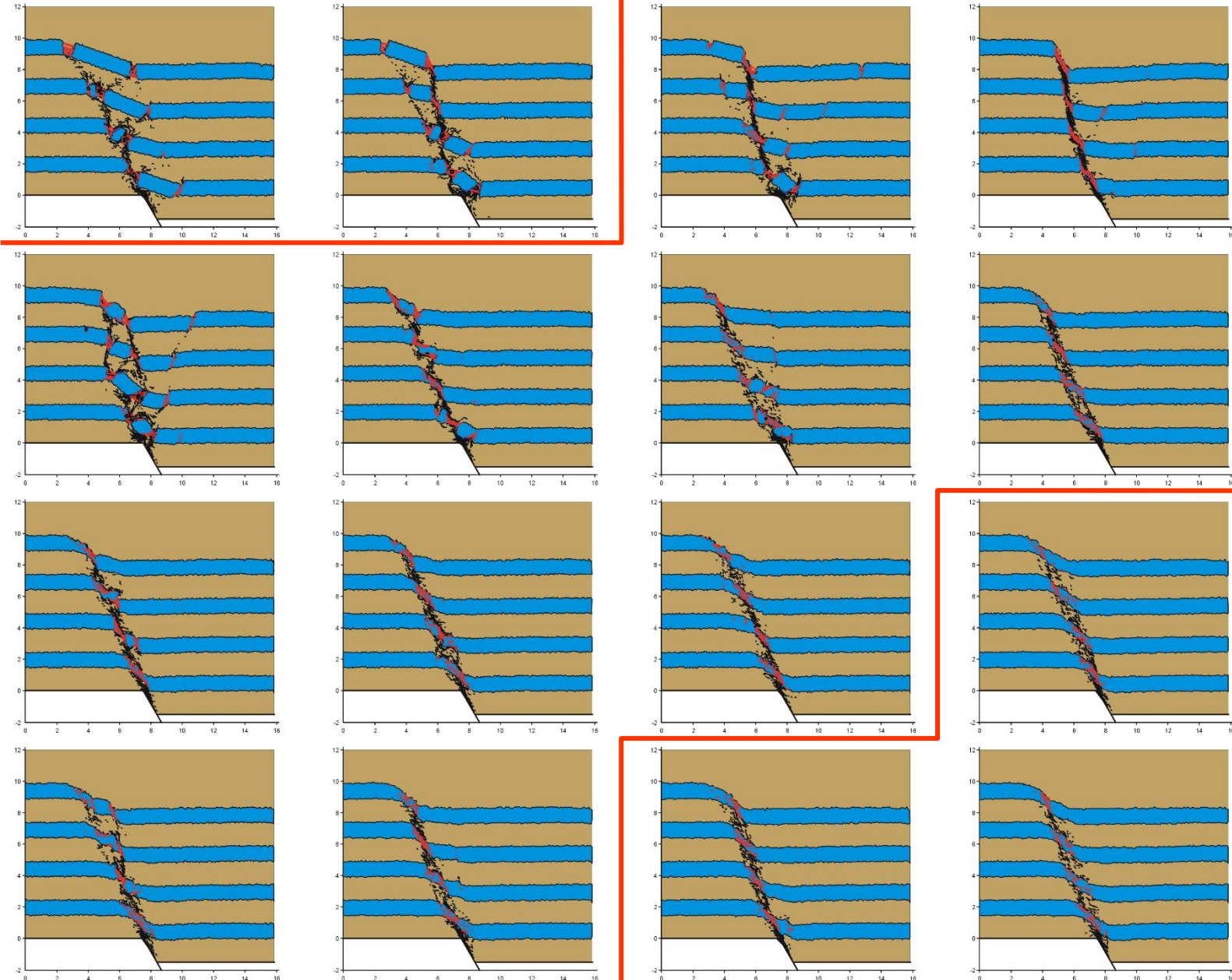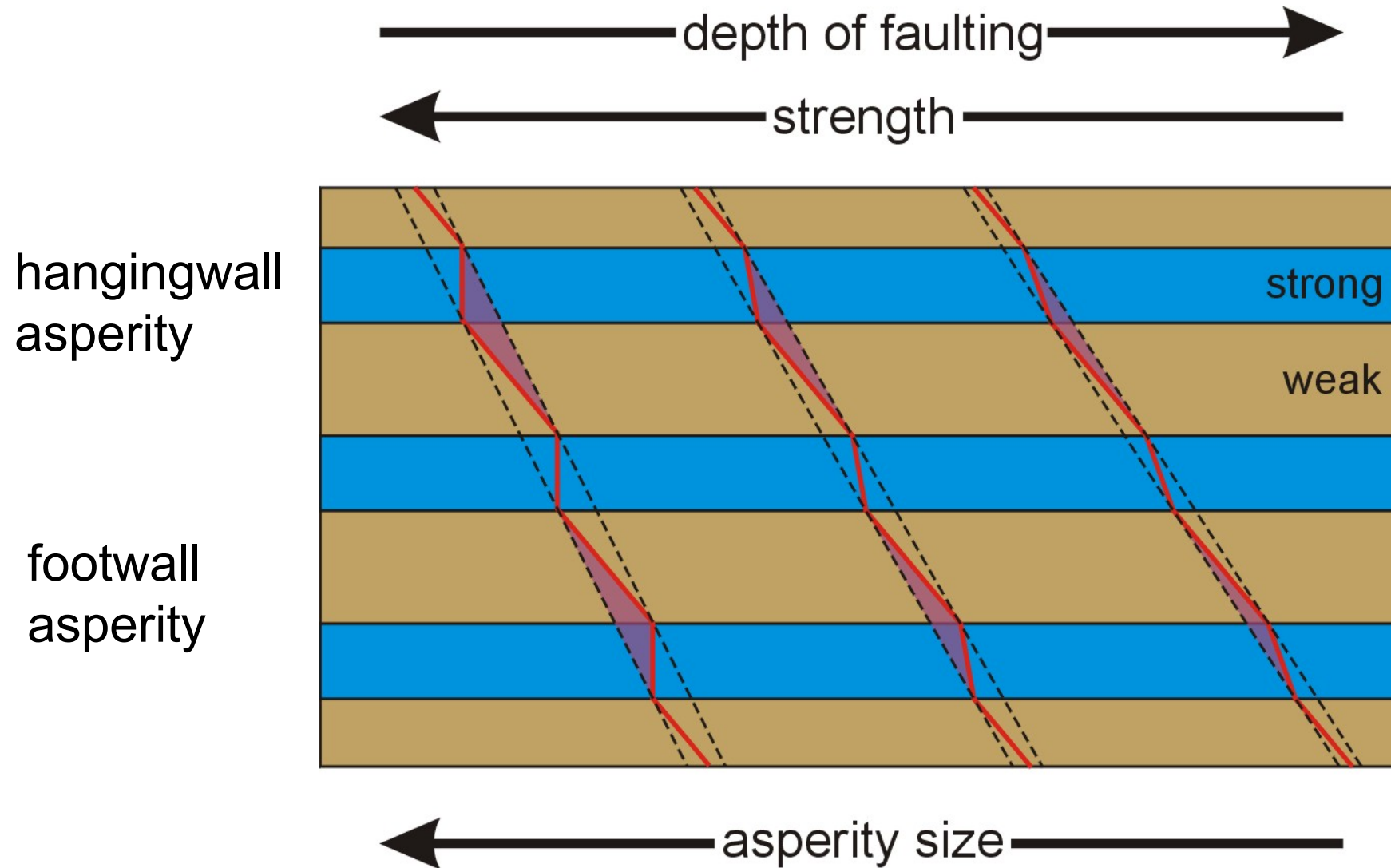
throw = 2.0 m

unconfined compressive strength

Schöpfer et al. (2007)

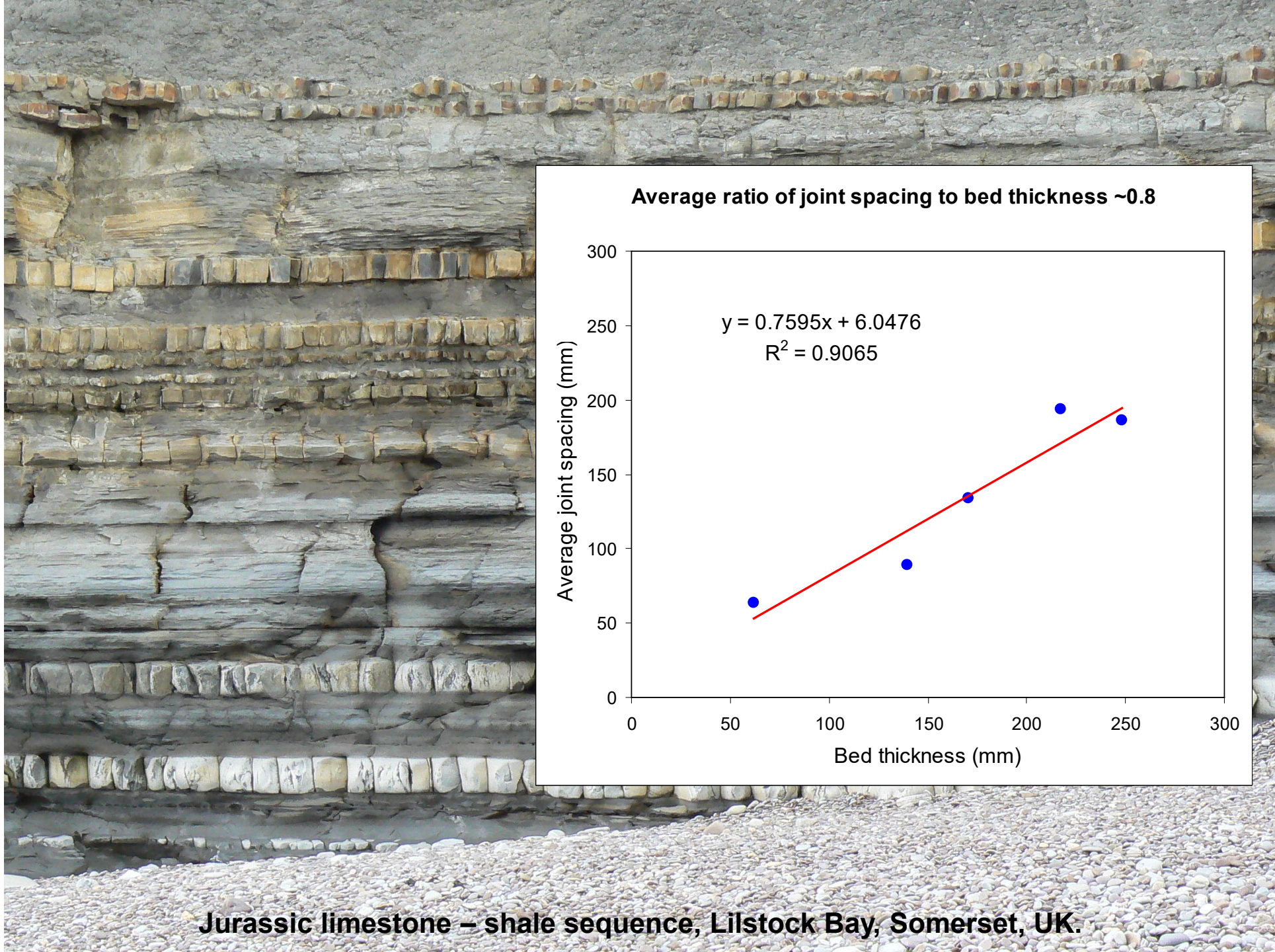# Impact of fault dip variation on asperity size and consequently fault rock width

Conclusions (1)

- Fault zone complexities are a function of strength contrast and depth of faulting.

- Faulting at low confining pressure is characterised by Mode I fracturing of the strong layers which leads to a staircase geometry (fault dip refraction).

- With increasing depth of faulting or decreasing strength a transition from Mode I to shear failure occurs (hybrid shears). This transition leads to a decrease of fault dip in the strong layers and an associated decrease in fault zone complexity.
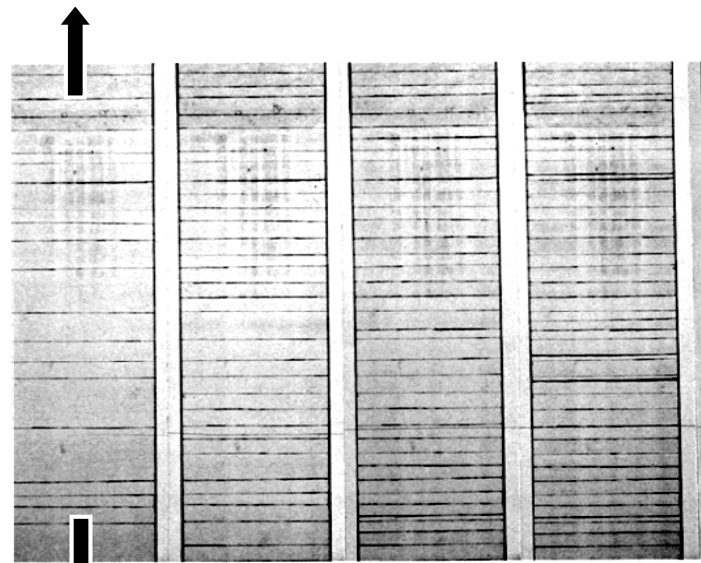
Rock joints

Jurassic limestone – shale sequence, Lilstock Bay, Somerset, UK.

Average ratio of joint spacing to bed thickness ~0.8

$y = 0.7595x + 6.0476$
$R^2 = 0.9065$

Average joint spacing (mm) vs Bed thickness (mm)

Jurassic limestone – shale sequence, Lilstock Bay, Somerset, UK.
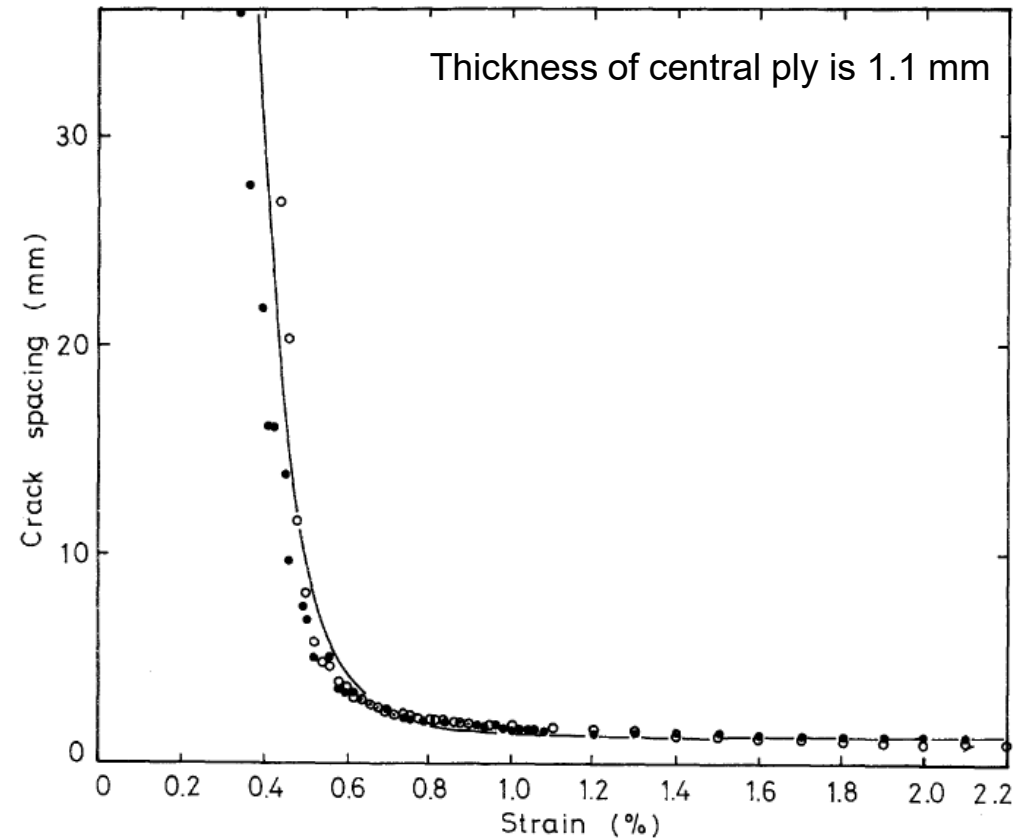
Fractures in glass fibre / epoxy resin laminates

← 'Map view' fracture evolution

(a) 0.56 (b) 0.72 (c) 0.90 (d) 1.10

(e) 1.30 (f) 1.70 (g) 1.90 (h) 2.40

20 mm

Fracture spacing vs layer parallel strain

Thickness of central ply is 1.1 mm
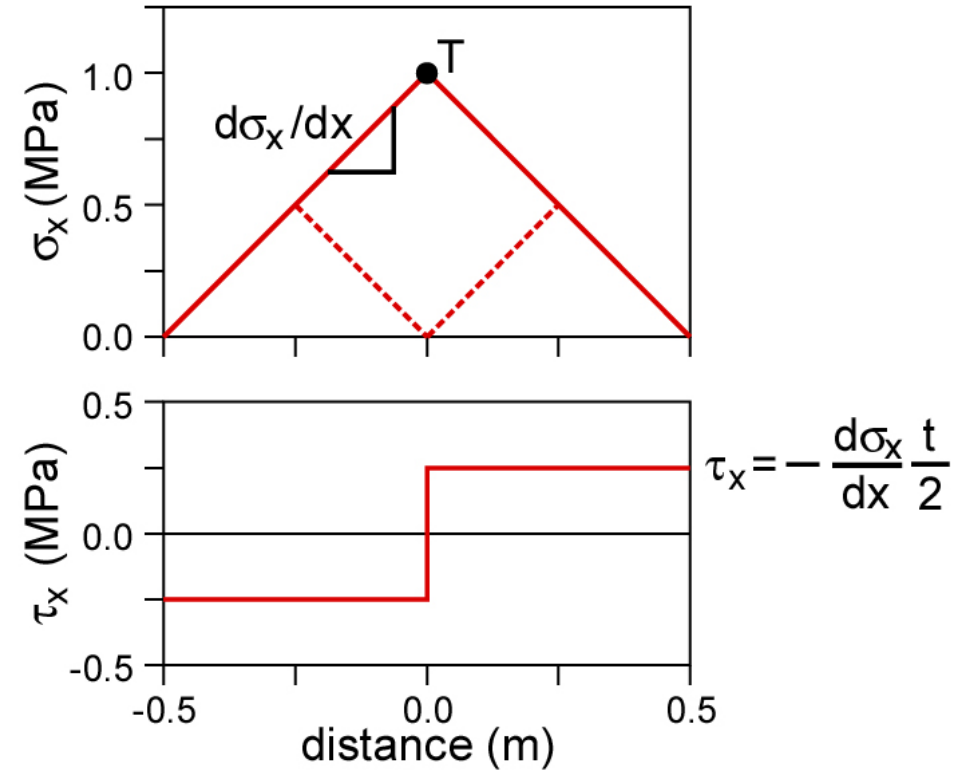
Manders et al. (1983)

Joint saturation: The full-slip model

(N.J. Price, 1966)

$$\frac{s_c}{t} = \frac{T}{\tau}$$

$$\tau_x = -\frac{d\sigma_x}{dx}\frac{t}{2}$$
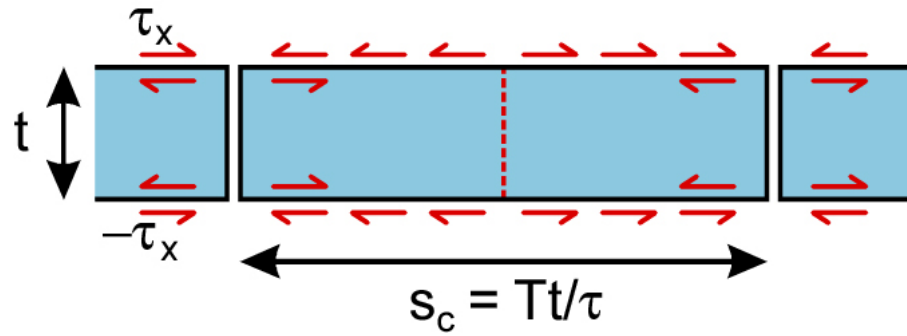
Example

T = 1 MPa, τ = 0.25 MPa

$s_c / t = 4$

hence $s_{min} / t = 2$

Schöpfer et al. (2011)

Verification of full-slip model with plane-strain FEM model

E = 10 GPa, ν = 0.25, σ_{yy} = 1 MPa

τ = 0.25 MPa
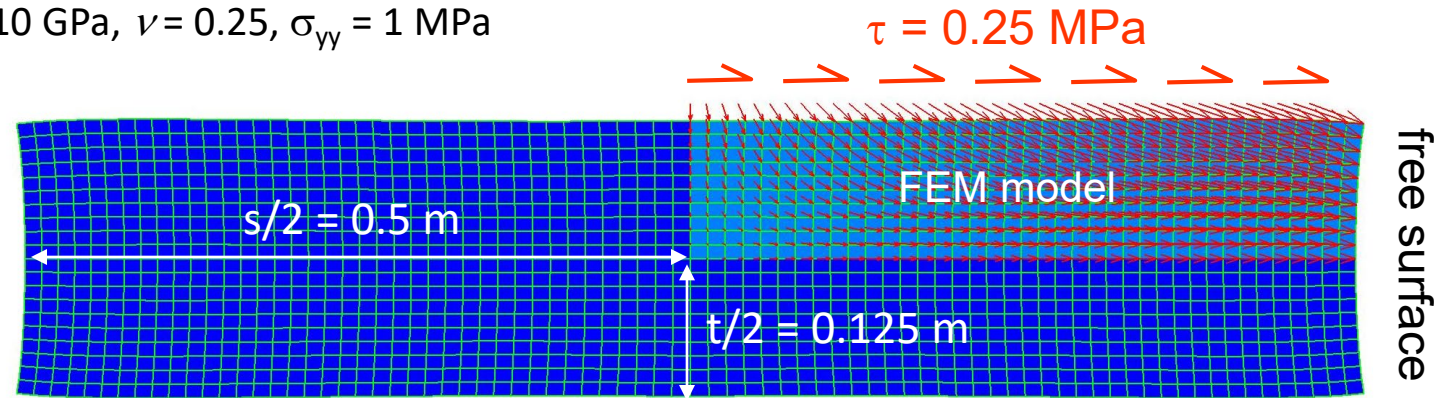
Displacements x 1000 (low resolution model)
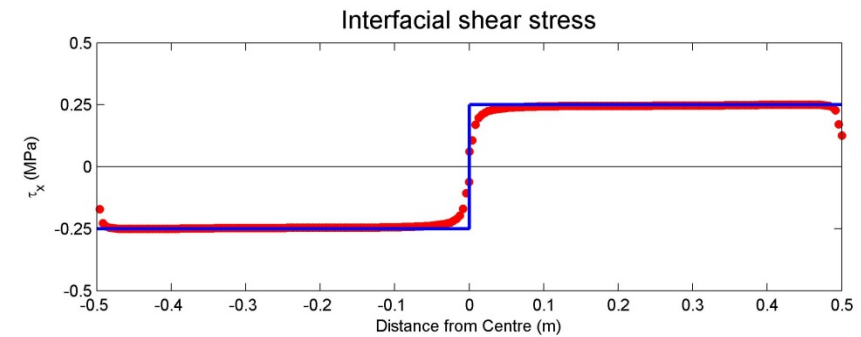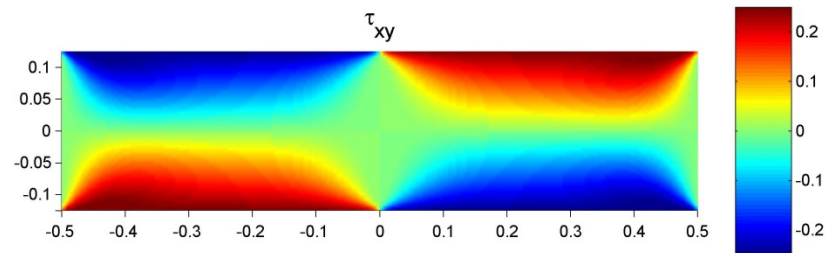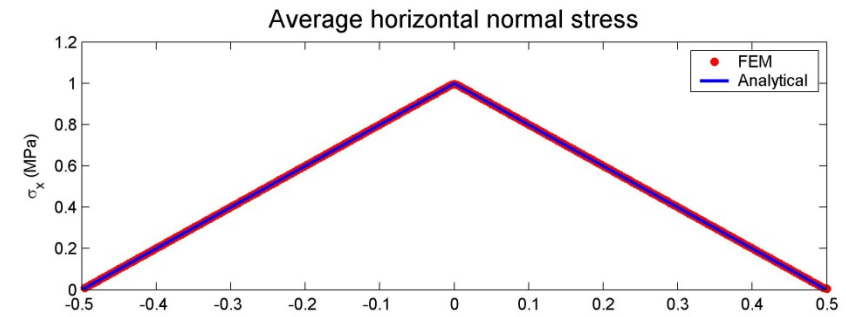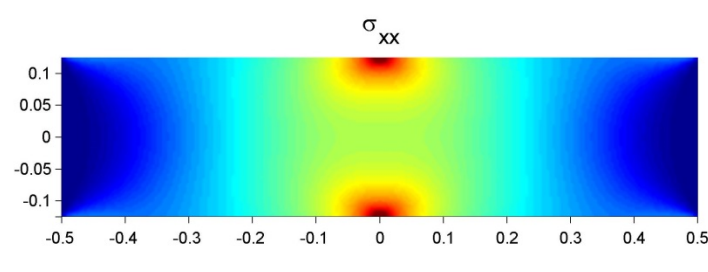
FEM Models run with code described in:
Alberty et al. (2002). Matlab Implementation of the Finite Element Method in Elasticity. Computing 69, 239–263

Joint saturation: Compressive Stress Criterion

(Altus & Ishai, 1986; Schoeppner & Pagano, 1999)
Stress-Transition Theory (Bai & Pollard, 2000)

$t = d = 0.25$ m,
$E_f = 10$ GPa, $E_m = 3.33$ GPa,
$v_f = v_m = 0.25$
$e = 0.005$, $P_{conf} = 2$ MPa

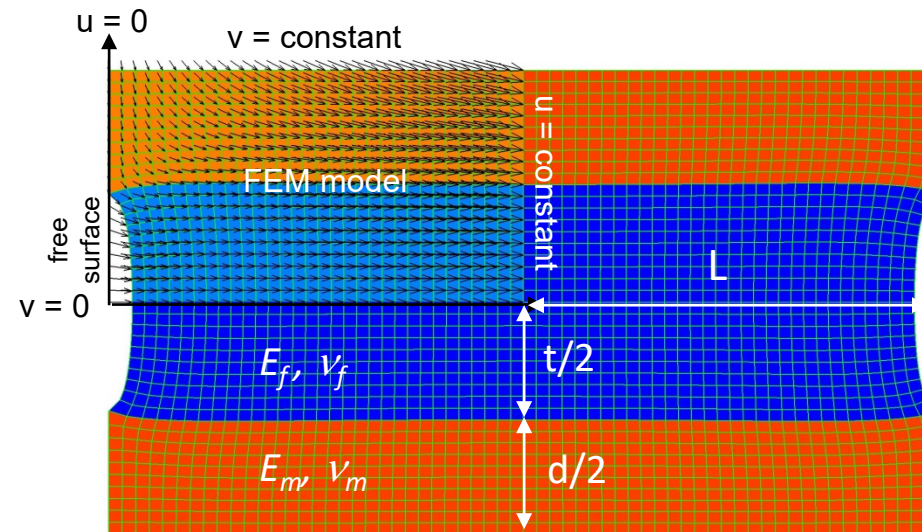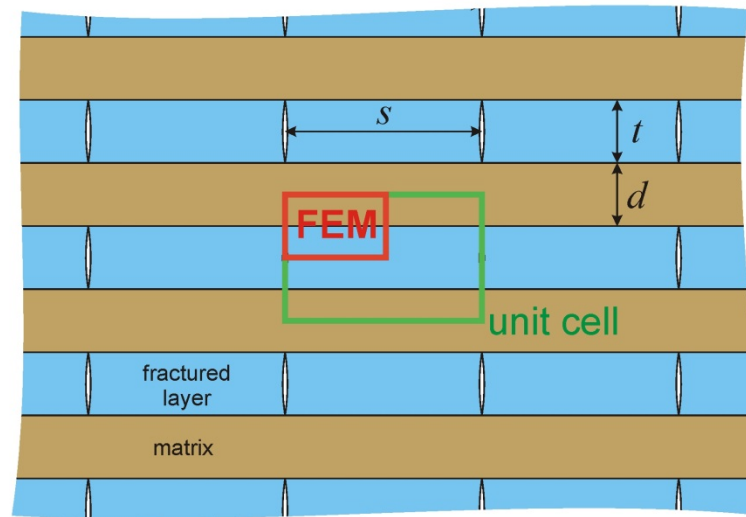Displacements x 20 (low resolution model)

FEM Models run with code described in:
Alberty et al. (2002). Matlab Implementation of the Finite Element Method in Elasticity. Computing 69, 239–263

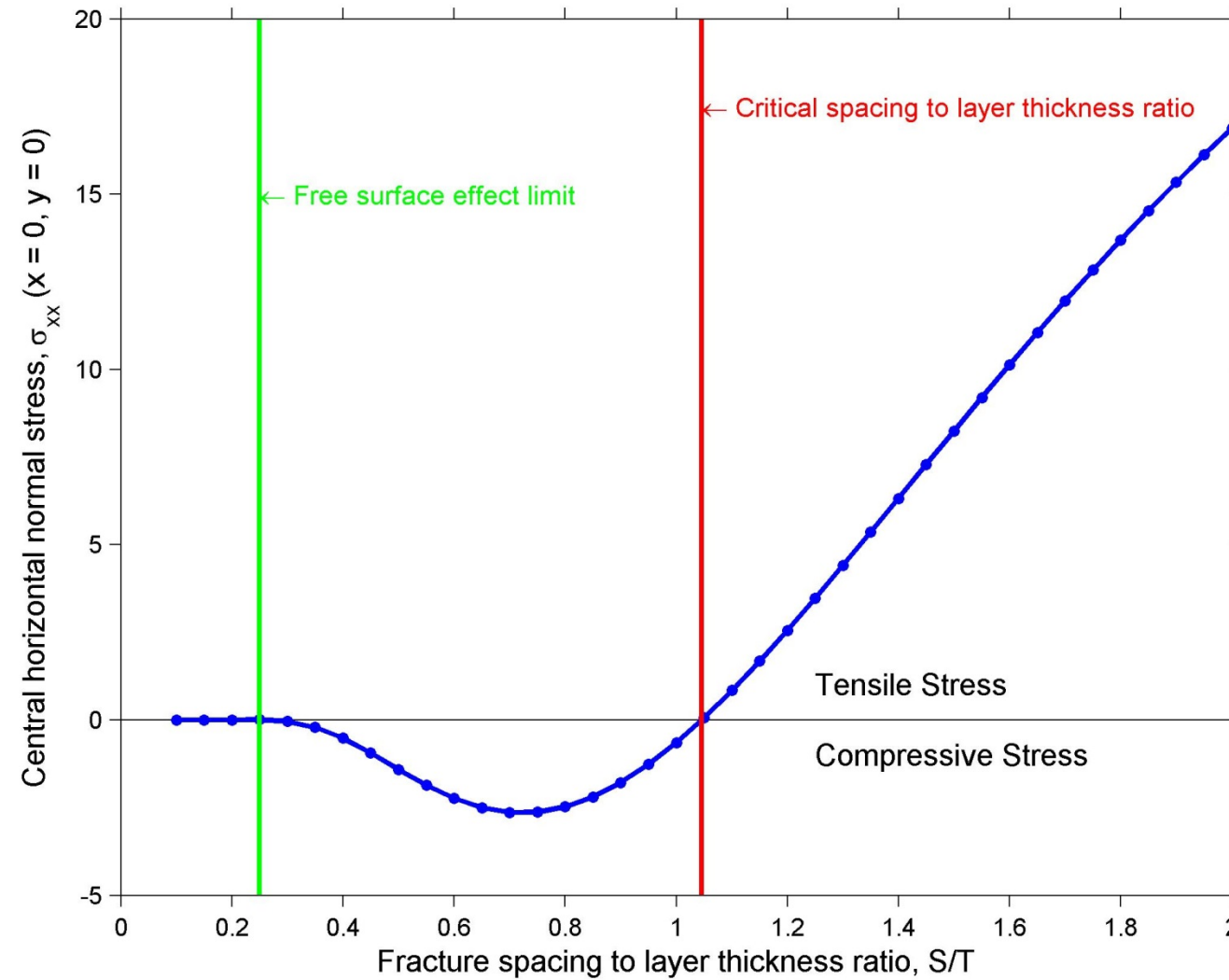# Horizontal normal stress distribution within a fracture-bound block
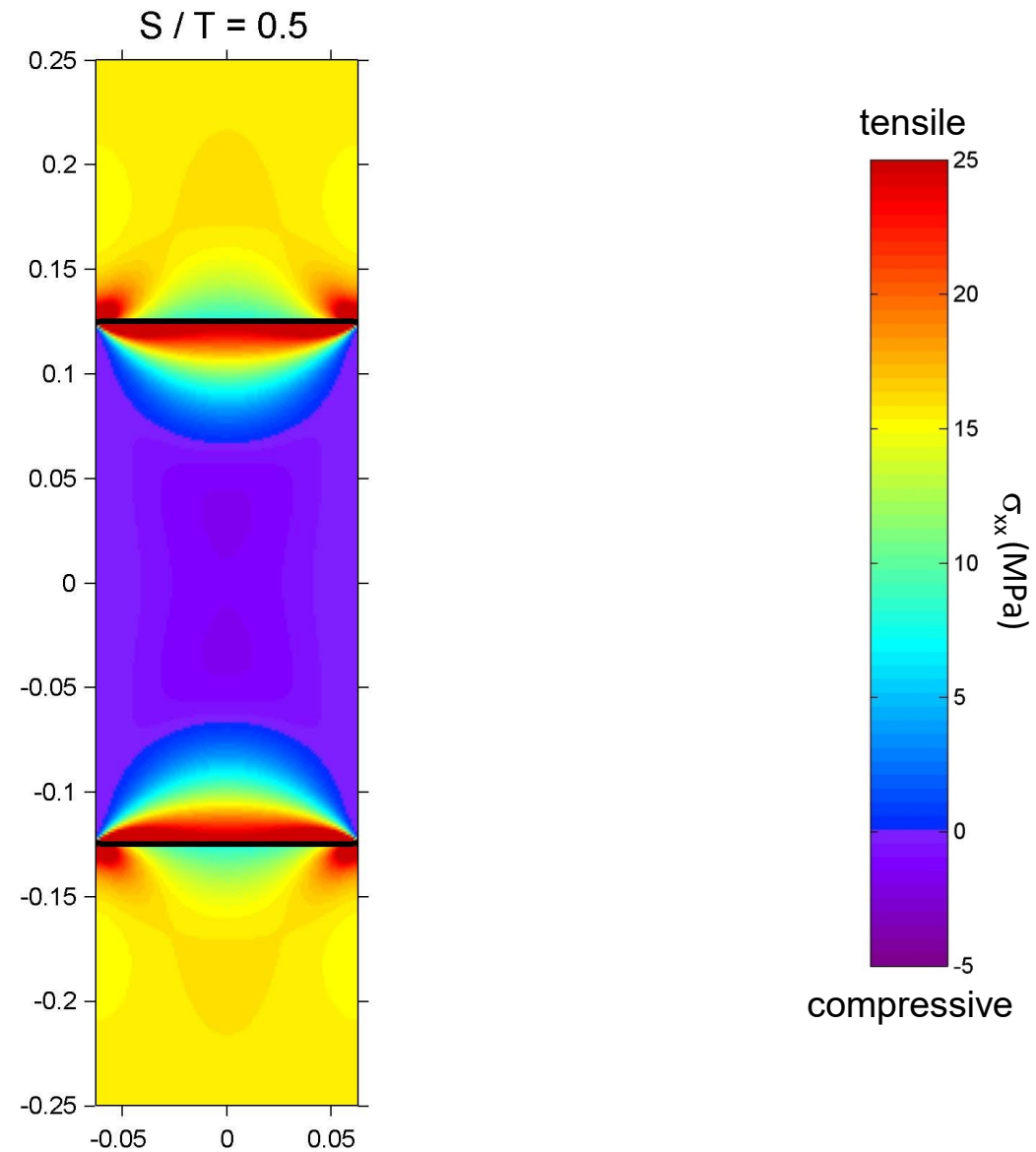
S / T = 0.5

FEM Models run with code described in:
Alberty et al. (2002). Matlab Implementation of the Finite Element Method in Elasticity. Computing 69, 239–263

Compressive Stress Criterion

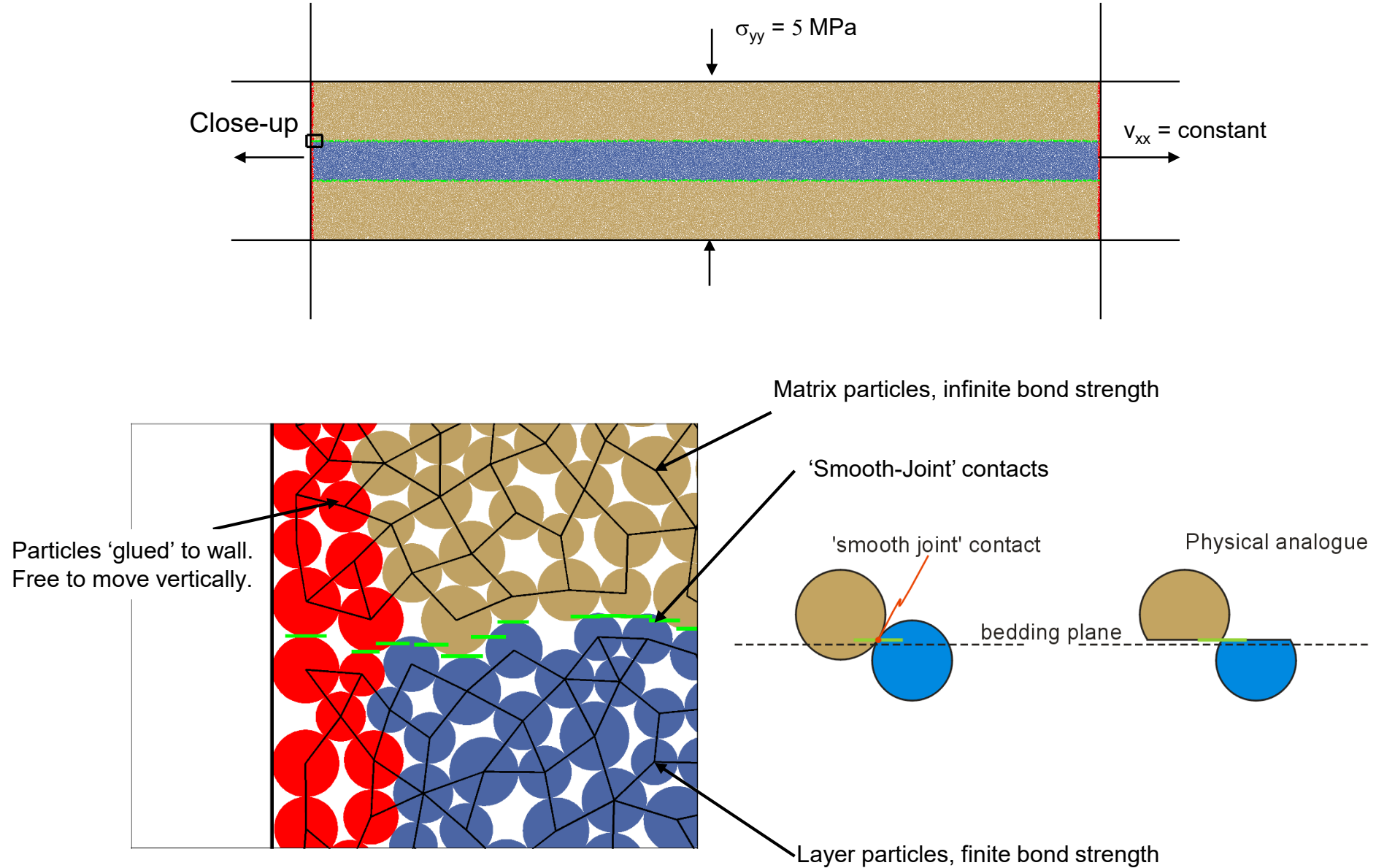## Based on horizontal stress within centre of fracture-bound block
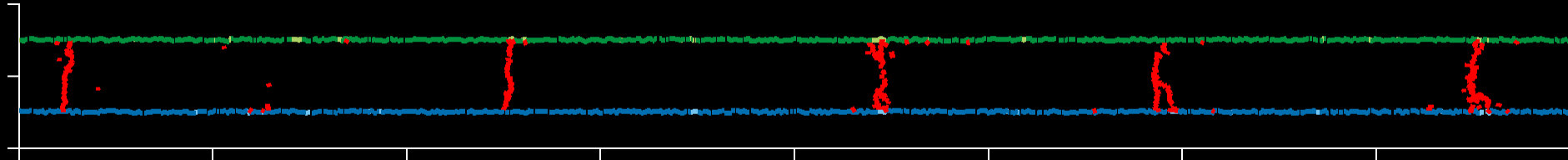

(see also Bai et al., 2000)

Two theories for joint saturation spacing

- The **1-D full-slip model** predicts that the maximum fracture spacing / layer thickness ratio (s/t) is equal to ratio of layer tensile strength to interface shear strength (T/τ). Full-slip models hence offer an explanation for fracture saturation.

- In **2-D continuum models without interfacial slip** a through-going central belt of layer-parallel compressive normal stress develops in-between the fractures at a fracture spacing to layer thickness ratio of ~1.0. This compressive stress is interpreted to inhibit further fracture growth and is hence used as an explanation for joint saturation.
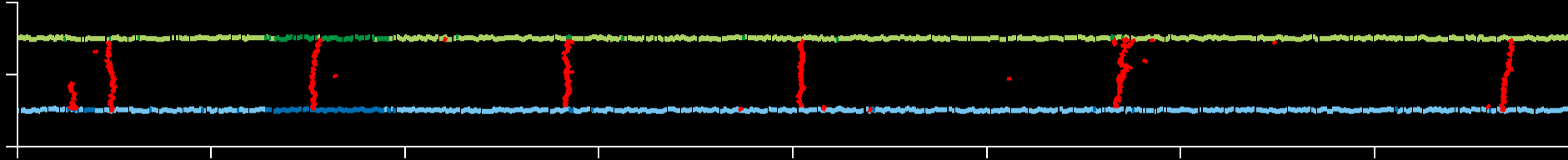
Boundary conditions for *PFC2D* jointing models

σ_{yy} = 5 MPa

Close-up

v_{xx} = constant

Matrix particles, infinite bond strength

'Smooth-Joint' contacts

Particles 'glued' to wall.
Free to move vertically.

'smooth joint' contact

Physical analogue

bedding plane

Layer particles, finite bond strength

Schöpfer et al. (2011)

μ = 0.2
s/t = 3.24 − 6.48

μ = 0.3
s/t = 2.16 − 4.32

μ = 0.5
s/t = 1.30 − 2.60

μ = 0.8
s/t = 0.81 − 1.62

Schöpfer et al. (2011)
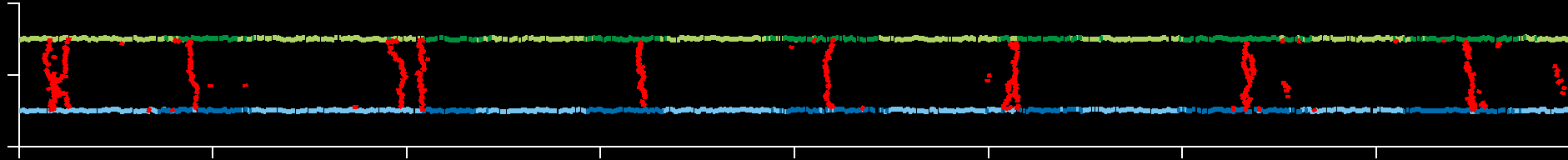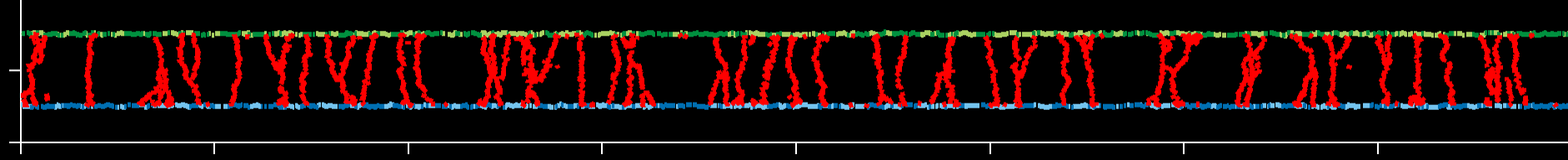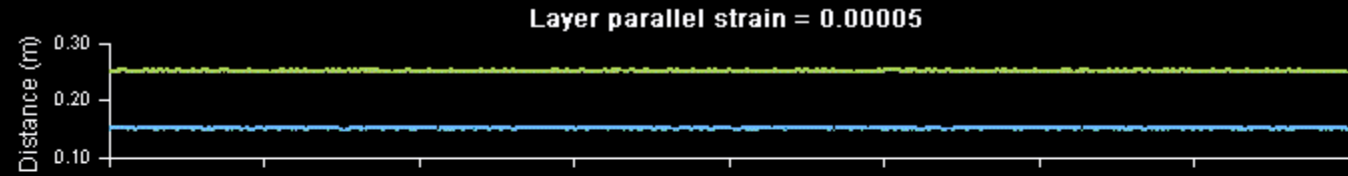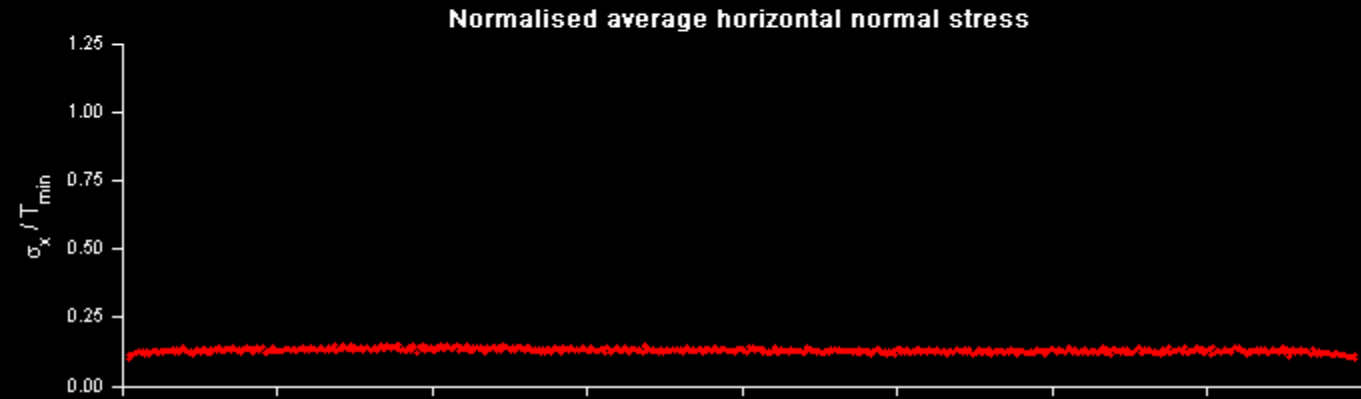
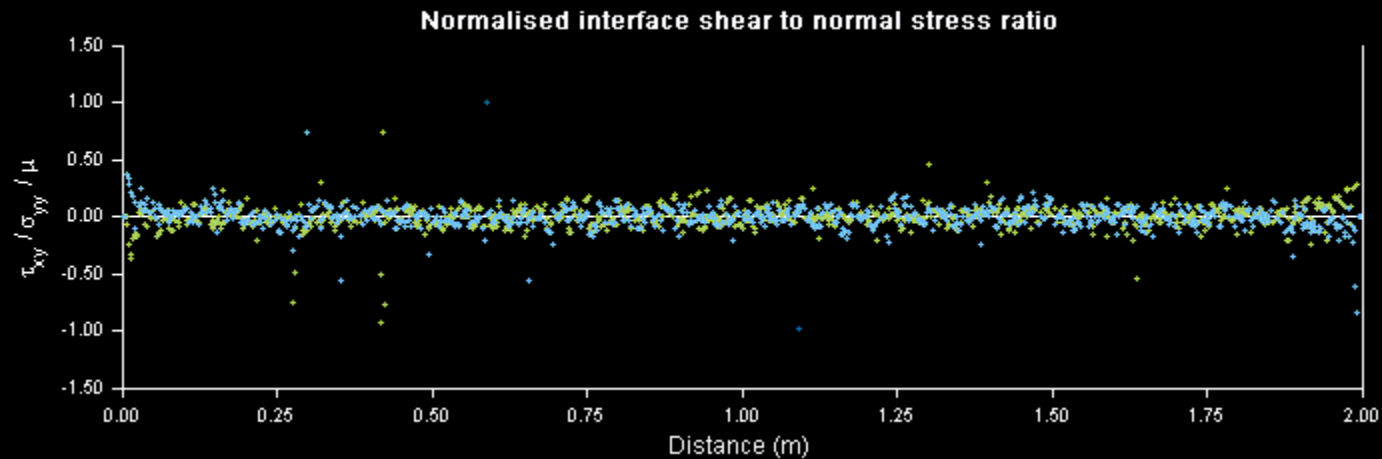# Animation illustrating jointing and associated stress evolution

Model in physical space

Average layer-parallel normal stress, normalized by layer's tensile strength
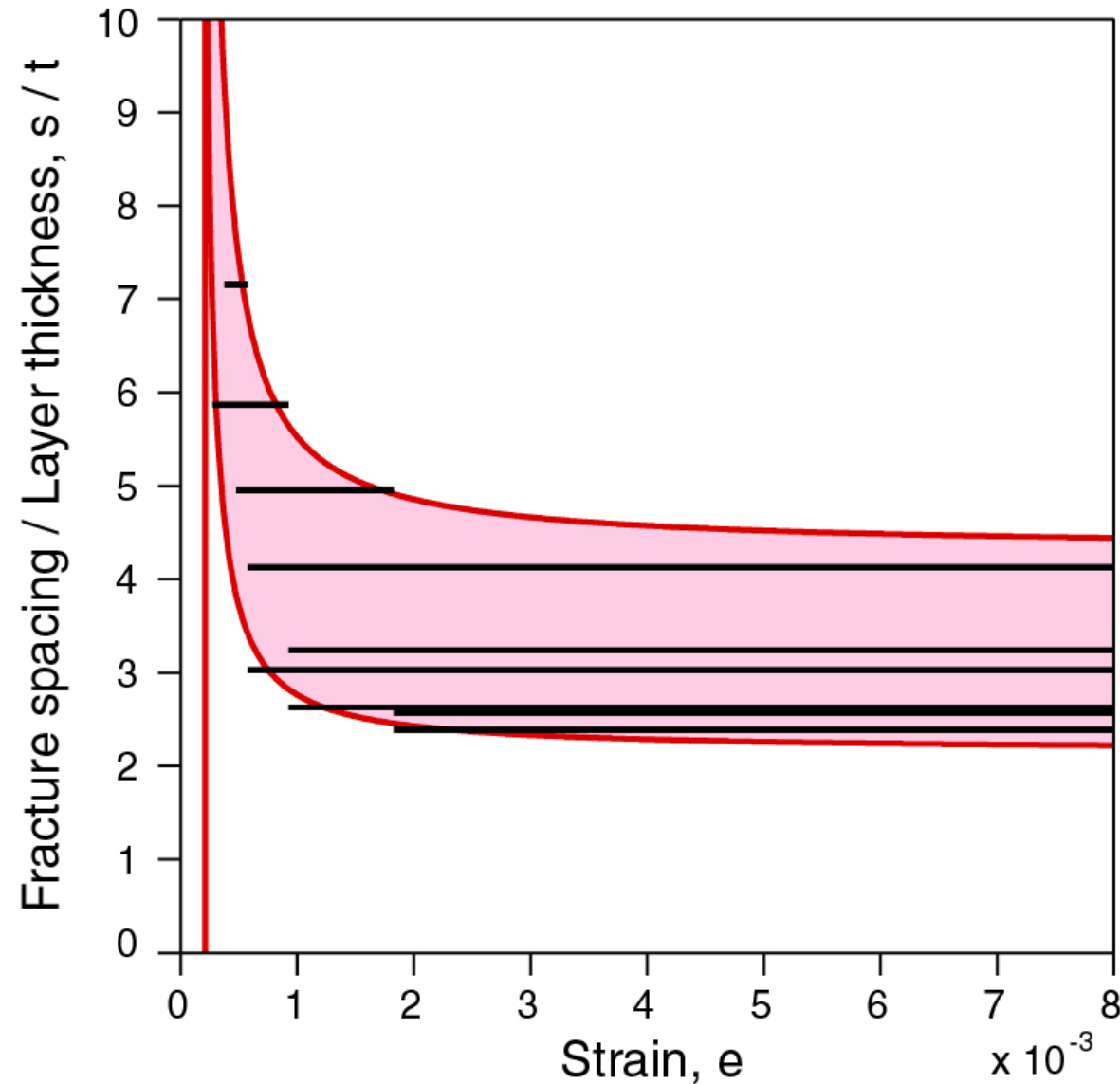
Interfacial shear to normal stress ratio, normalized by friction coefficient

$\mu = 0.2$
s/t = 3.24 – 6.48

Layer parallel strain = 0.00005

Normalised average horizontal normal stress

Normalised interface shear to normal stress ratio

Fracture spacing evolution in *PFC2D* model ($\mu = 0.3$)

s/t-range under full-slip conditions: 2.16 – 4.32

Model fracture spacing data (black lines) are compared with a 1D shear lag analytical solution (red lines and pink patch).

Schöpfer et al. (2011)

μ = 0.2
s/t = 3.24 − 6.48

μ = 0.3
s/t = 2.16 − 4.32

μ = 0.5
s/t = 1.30 − 2.60
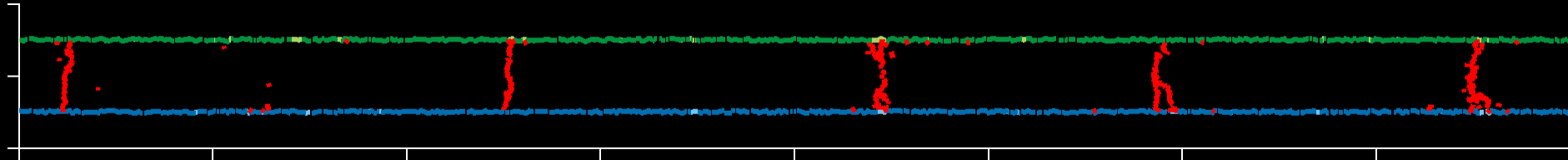
μ = 0.8
s/t = 0.81 − 1.62

Schöpfer et al. (2011)

Fracture spacing evolution in *PFC2D* model (μ = 0.8)

s/t-range under full-slip conditions: 0.81 – 1.62
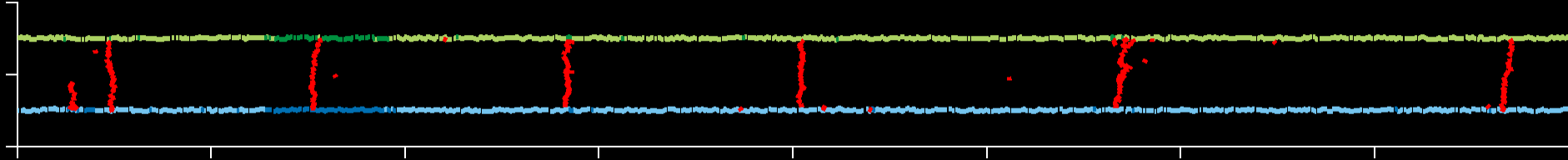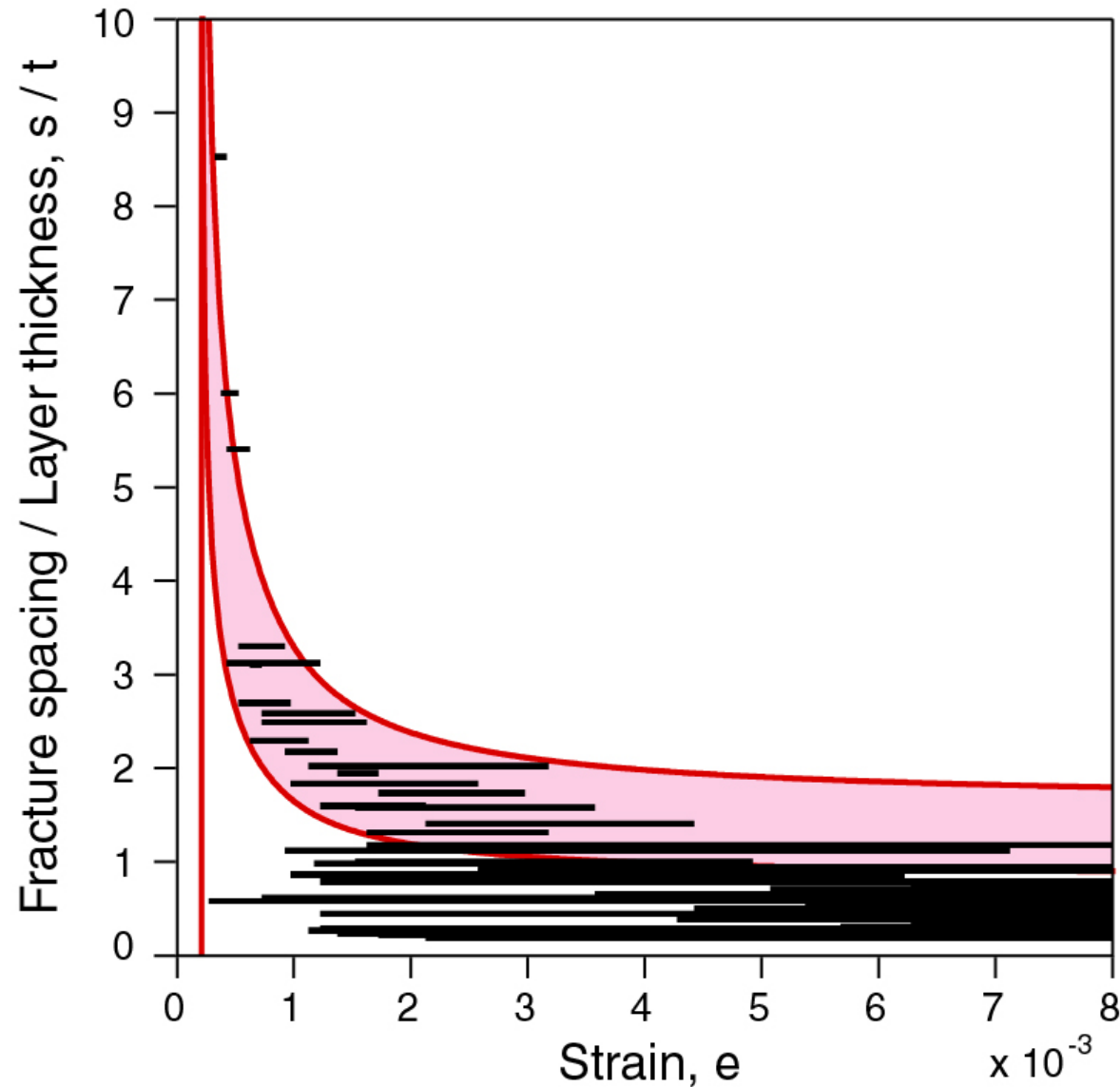

Model fracture spacing data (black lines) are compared with a 1D shear lag analytical solution (red lines and pink patch).
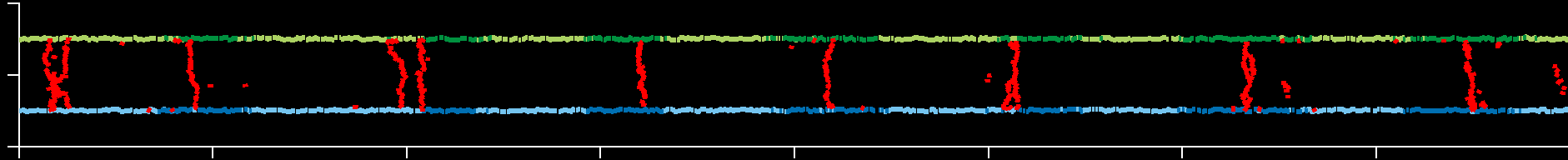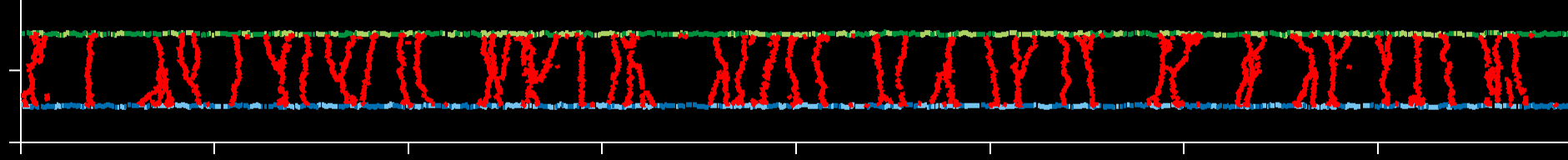
Schöpfer et al. (2011)

Formation of infill fractures in μ = 0.8 model

e = 0.00560

1D full-slip prediction for
μ = 0.8
s/t = 0.81 − 1.62

horizontal normal stress, σ_{xx} (MPa)

s / t = 0.9

Formation of infill fractures in $\mu = 0.8$ model

e = 0.00565

1D full-slip prediction for
μ = 0.8
s/t = 0.81 − 1.62

horizontal normal stress, σ_{xx} (MPa)

Schöpfer et al. (2011)

Formation of infill fractures in μ = 0.8 model

e = 0.00625

1D full-slip prediction for
μ = 0.8
s/t = 0.81 − 1.62

horizontal normal stress, σ_{xx} (MPa)

s / t = 0.6 & s / t = 0.3

Schöpfer et al. (2011)
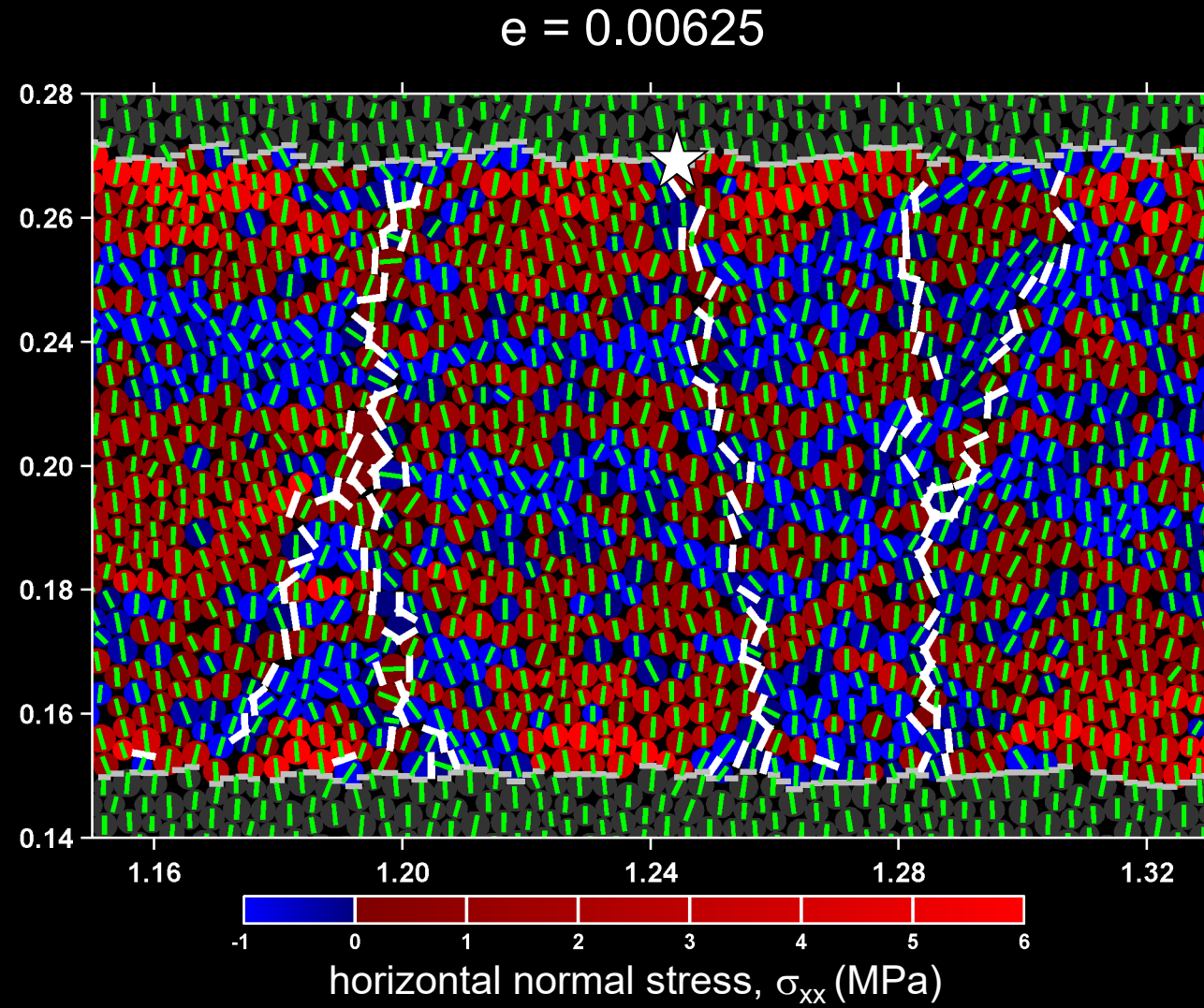
Normalised fracture spacing vs interface friction

PFC2D model data at fracture saturation (e = 0.008)

Schöpfer et al. (2011)
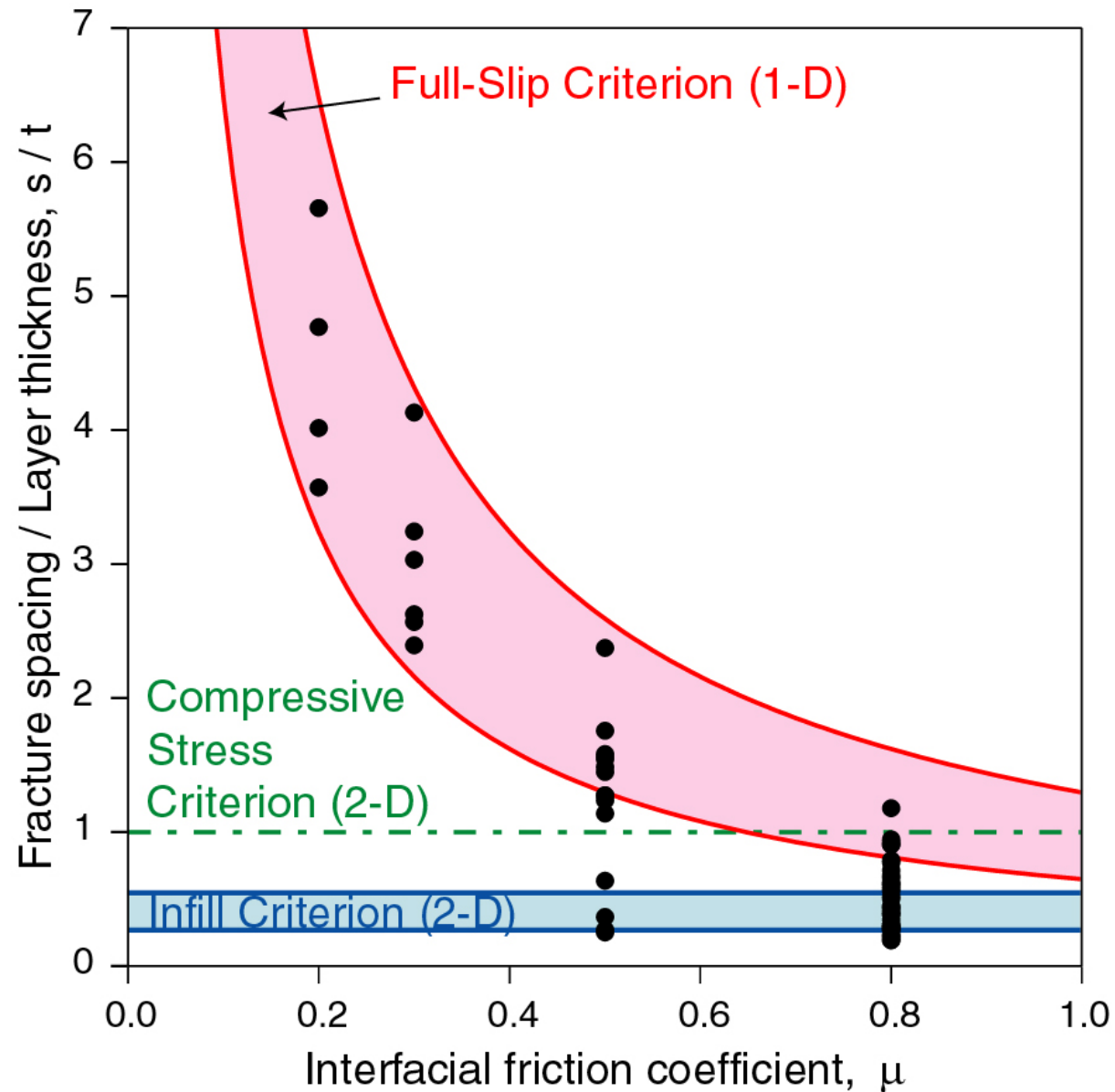
Conclusions (2)

• The validity and consequent applicability of 1-D models depends on the ratio of layer tensile strength to interface shear strength (T/τ).

• High T/τ ratios (ca. >3.0 in our models) promote interfacial slip and yield results that provide an excellent fit to a 1-D shear lag model.

• At lower strength ratios interfacial slip is suppressed and the heterogeneous 2-D stress distribution within fracture-bound blocks controls further fracture nucleation (e.g., infill fractures).

Creep of rock salt

Isoclinal folds in naturally deformed rock salt (Hallstatt salt mine)
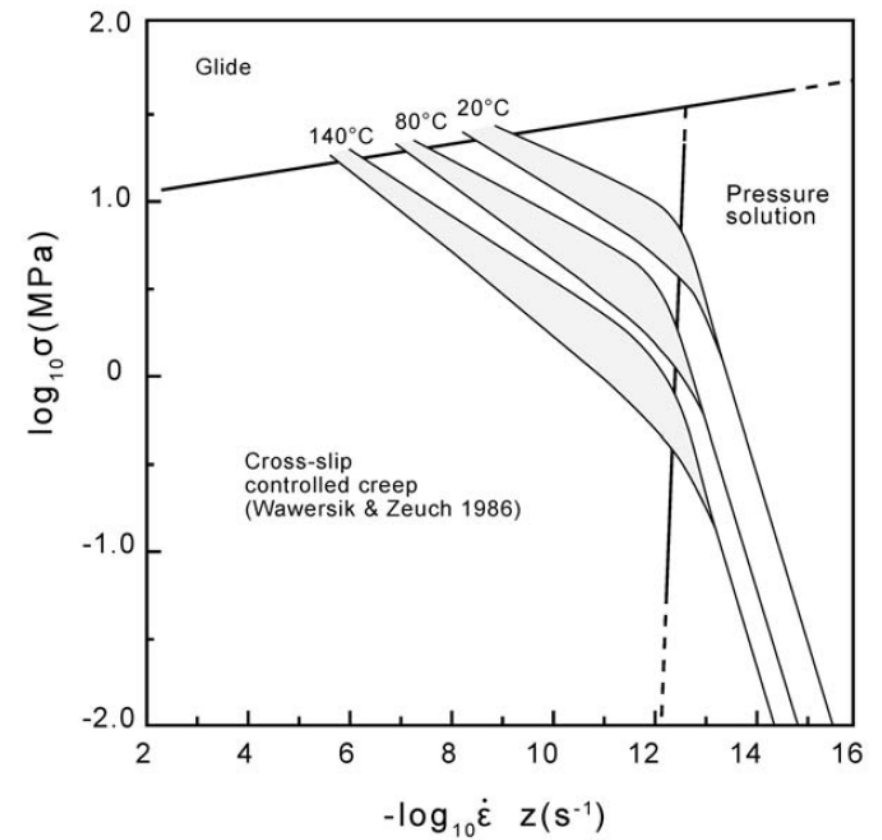
Deformation mechanism map for dense rock salt, incorporating solution-precipitation creep for a grain size d = 10 mm. (Urai et al., 2008)
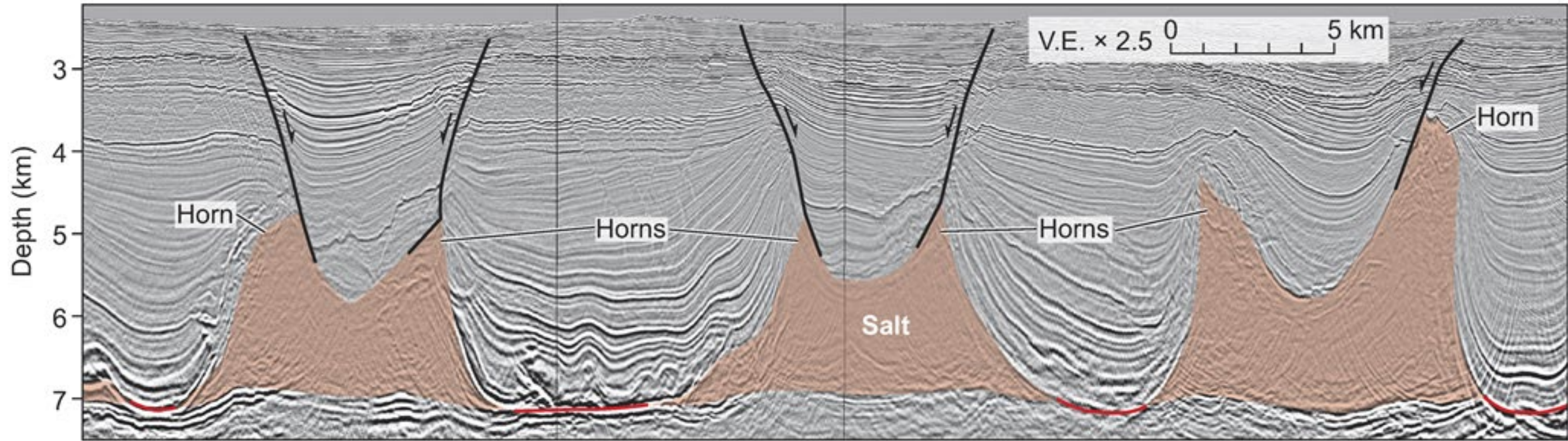
Salt tectonics modelling

Sedimentary overburden deforms in a brittle fashion (faulting) → *PFC2D*

Salt deforms by viscous creep → *FLAC (with creep option)*

During extensional diapir fall, crestal fault blocks indent the tops of diapirs. Relict salt forms horns on either side of an indenting graben. Campos basin seismic data courtesy of PGS (from Hudec & Jackson, 2017).
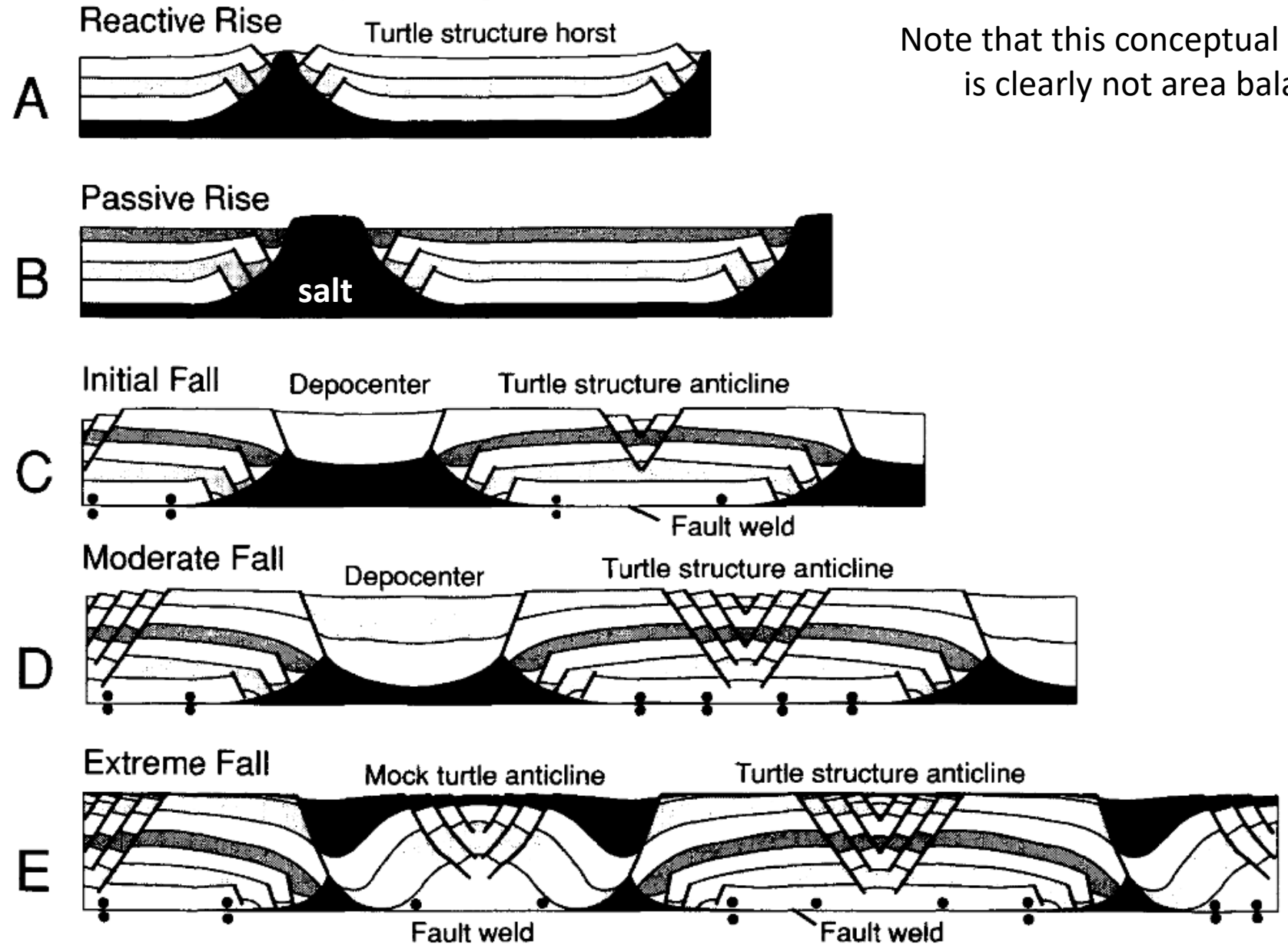
Turtle structure horsts, turtle structure anticlines and mock-turtle anticlines

Rise and fall of diapirs during sedimentation.

Three types of extensional turtle structure successively form:

(1) Turtle structure horsts;

(2) Turtle structure anticlines;

(3) Mock turtle* anticlines.

Mock turtle in Alice in Wonderland

Note that this conceptual model is clearly not area balanced!

A Reactive Rise — Turtle structure horst

B Passive Rise — salt

C Initial Fall — Depocenter — Turtle structure anticline — Fault weld

D Moderate Fall — Depocenter — Turtle structure anticline

E Extreme Fall — Mock turtle anticline — Turtle structure anticline — Fault weld — Fault weld

Vendeville and Jackson (1992b)

Overview of coupled PFC2D-FLAC model for modelling salt tectonics
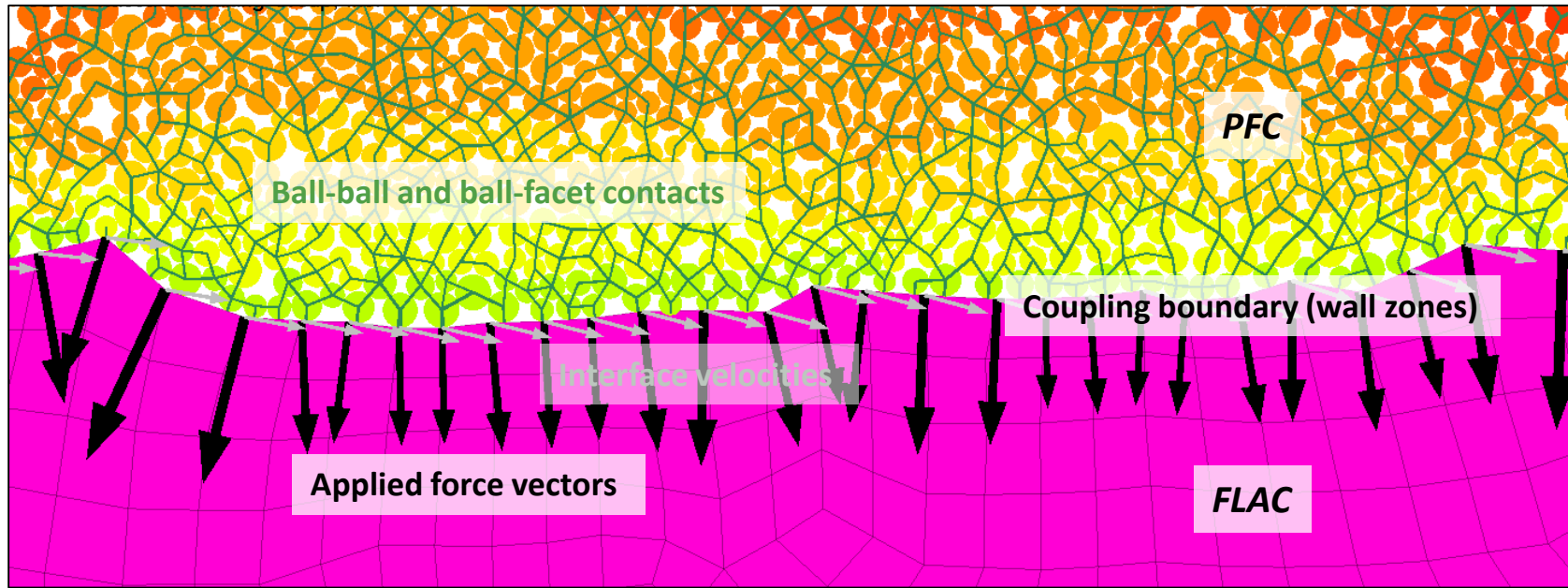
The sedimentary overburden is represented by circular particles that interact via a 'rolling friction' contact law.

Coupling is achieved via wall-zones.

The salt is idealized as a linear viscous material (Maxwell body) using the FLAC creep option.

The routine is a two-step process consisting of (1) 'sedimentation' and (2) 'salt flow':

1. The creep-time-step in FLAC is set to zero which enforces elastic behaviour. A layer of particles is generated and the DEM model is brought to mechanical equilibrium.
2. The creep-time-step in FLAC is set to a non-zero value so that viscous flow occurs. The creep-time-step is adjusted using a servo algorithm that keeps the out-of-balance force low. The salt flows for a duration that represents the geological time of the previously generated sedimentary layer. Automatic rezoning is used.

These two steps are repeated until the required geological time has elapsed.

Overview of geometrical and mechanical parameters of thin-skinned extension models

- Two layer system under constant layer parallel extension with initial salt thickness 1 km and a 500 m thick prekinematic overburden. Initial model length is 20 km.

- The total thickness of the two-layer system is kept constant via sedimentation.

- Models are run with linear viscous rheology ($\eta = 1 \times 10^{18}$ Pa s) and with the following (buoyant) densities*:

$$\rho'_s = 1200 \text{ kg/m}^3; \quad \rho'_o = 1200 \text{ kg/m}^3, \quad \rho'_o = 1450 \text{ kg/m}^3 \quad \text{or} \quad \rho'_o = 1700 \text{ kg/m}^3$$

- Strain rate and layer sedimentation interval are $\dot{e} = 7.9264 \times 10^{-15} \text{ s}^{-1} \quad \Delta t = 200{,}000 \text{ a}$
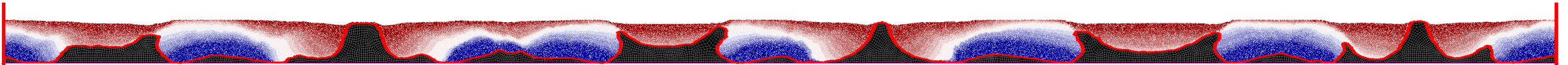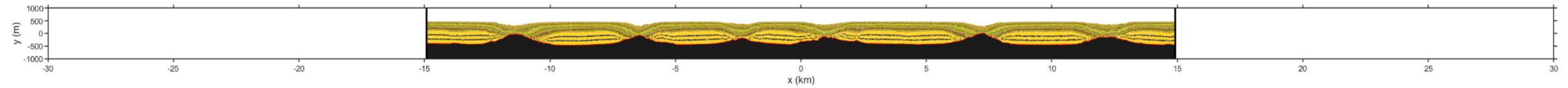

* Note that the 'packing porosity' of the particle model is ca. 15%. In order to achieve these buoyant material densities, the following particle densities are used: $\rho_p = 1412 \text{ kg/m}^3 \quad \rho_p = 1706 \text{ kg/m}^3 \quad \rho_p = 2000 \text{ kg/m}^3$

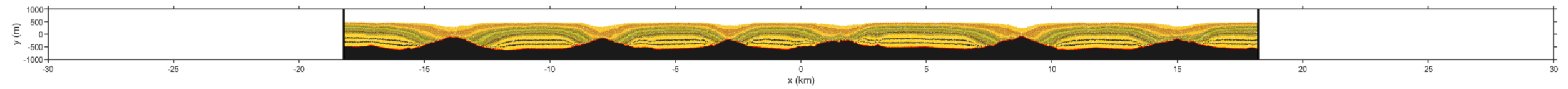# Constant strain rate extension with overburden buoyant density $\rho'_o = 1200 \, \text{kg/m}^3$

Constant strain rate extension with overburden buoyant density $\rho'_o = 1450\,\text{kg/m}^3$
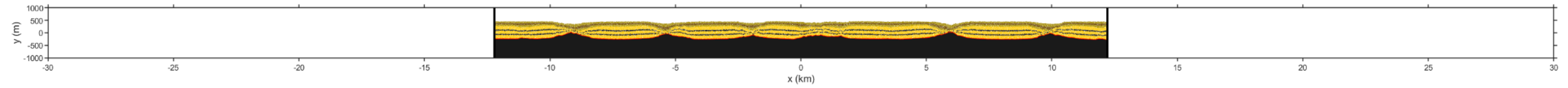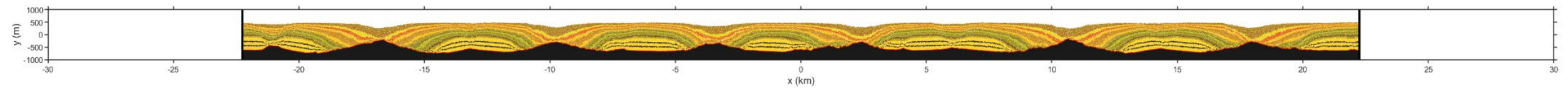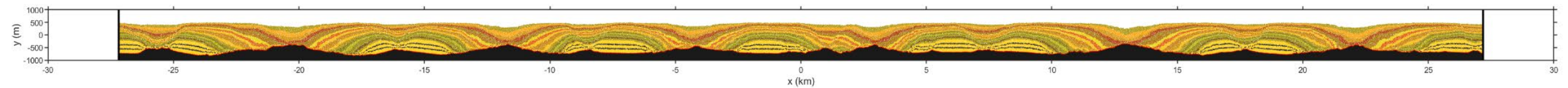

t = 0.80 Ma
$\beta = 1.22$

t = 1.60 Ma
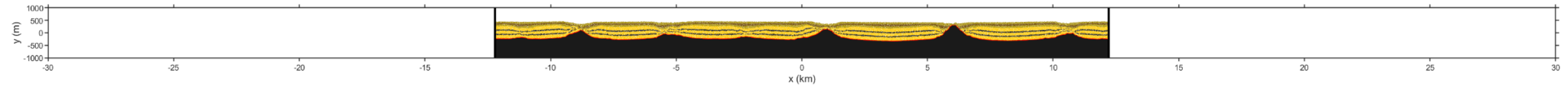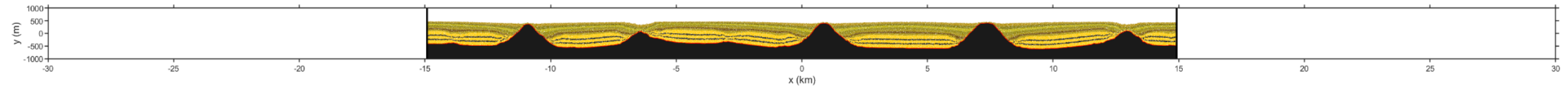$\beta = 1.49$

t = 2.40 Ma
$\beta = 1.82$

t = 3.20 Ma
$\beta = 2.23$

t = 4.00 Ma
$\beta = 2.72$

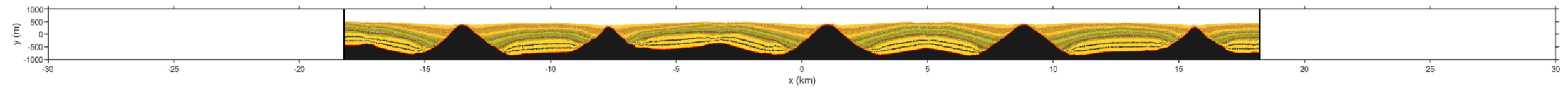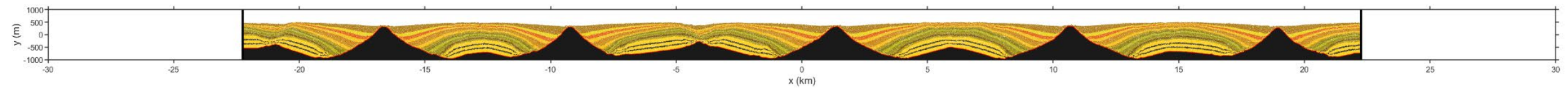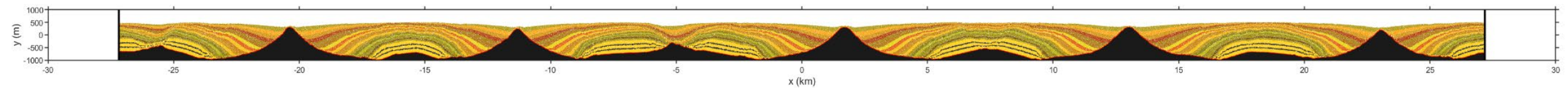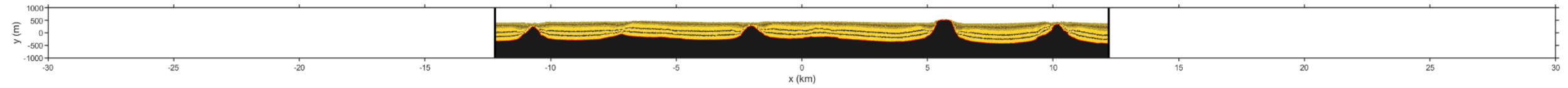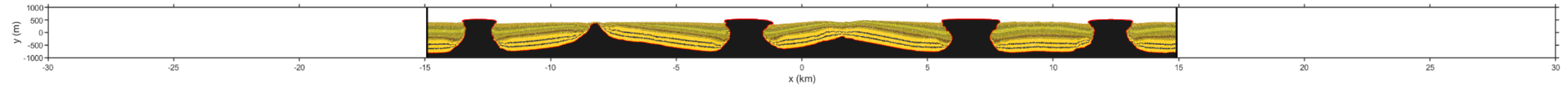# Constant strain rate extension with overburden buoyant density $\rho'_o = 1700 \, \text{kg/m}^3$

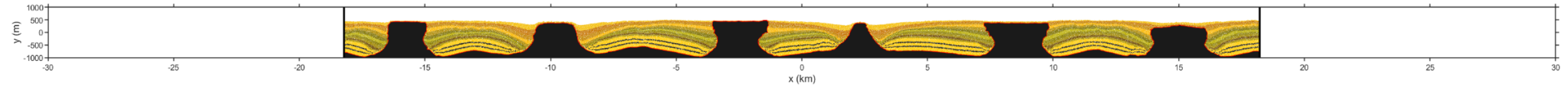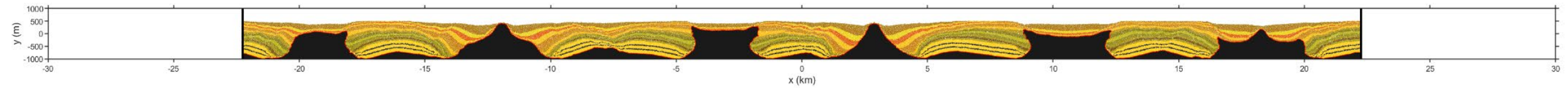t = 0.80 Ma
β = 1.22

t = 1.60 Ma
β = 1.49

t = 2.40 Ma
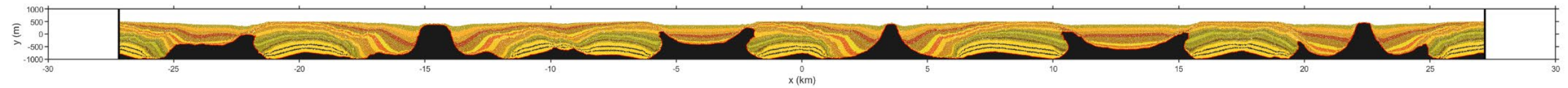β = 1.82
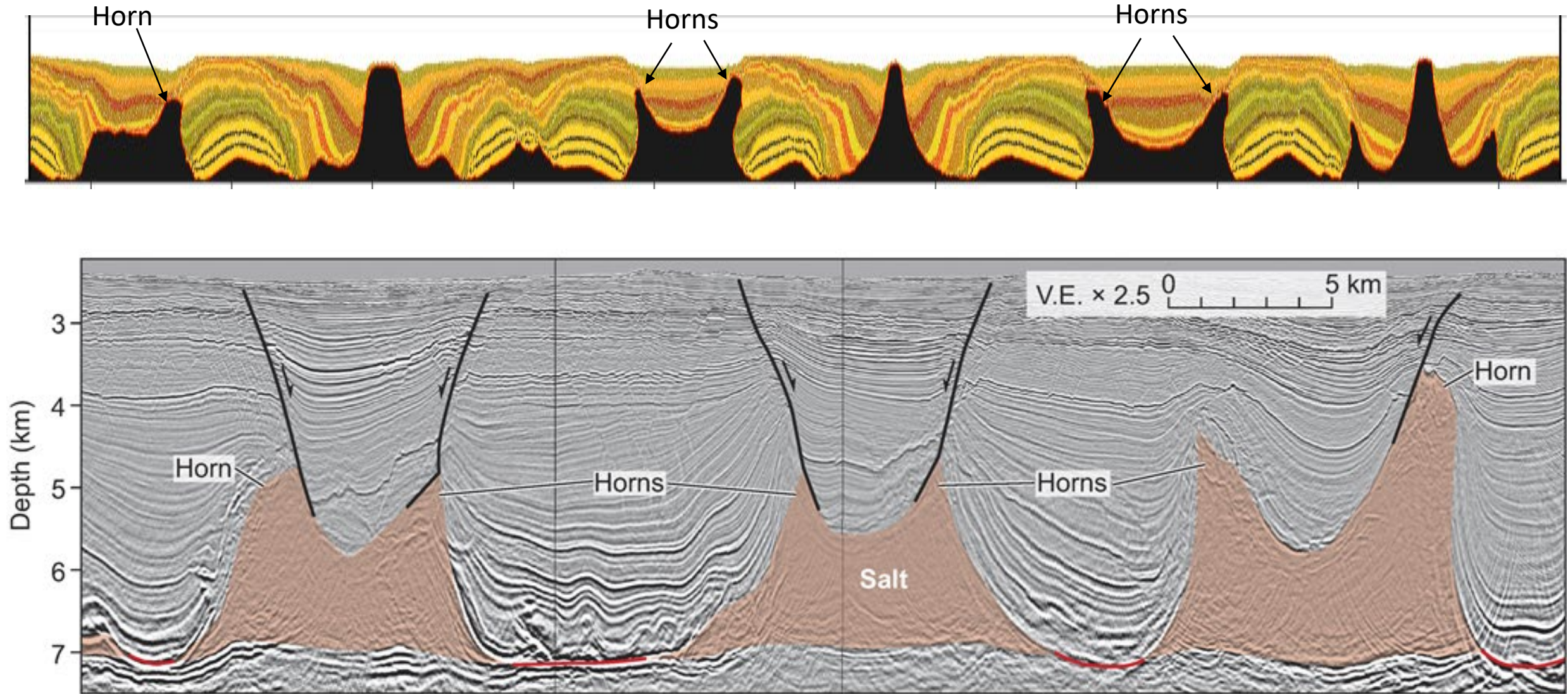
t = 3.20 Ma
β = 2.23

t = 4.00 Ma
β = 2.72

A qualitative comparison of coupled *PFC2D-FLAC* model and a natural example

Both model and seismic section are vertically exaggerated by a factor 2.5

Conclusions (3)

• A two-layer system comprised of a (linear) viscous substratum and a frictional plastic overburden subjected to layer-parallel stretching leads to necking instability.

• The density contrast between the overburden and substratum has (as expected) a profound impact on structural development.

• Certain details of the overburden structure and the sedimentary fill are strongly dependent on the initial positions of the diapirs (which due to the heterogeneous nature of the modelled overburden are not perfectly periodic!)

Summary

- Structural geologists should have a sound knowledge of geomechanics so that the mechanical genesis of rock structures can be better interpreted.

- Many existing analytical solutions from other disciplines (e.g., material sciences, civil engineering) can be adapted for problems related to structural geology.

- Numerical methods, such as the DEM or FLAC, are an excellent tool to forward model a wide range of rock structures.